A Zebrafish Model of Axenfeld-Rieger Syndrome Reveals That *pitx2* Regulation by Retinoic Acid Is Essential for Ocular and Craniofacial Development

Brenda L. Bohnsack,[1] *Daniel S. Kasprick,*[1] *Phillip E. Kish,*[1] *Daniel Goldman,*[2] *and Alon Kahana*[1]

Purpose. The homeobox transcription factor *PITX2* is a known regulator of mammalian ocular development, and human *PITX2* mutations are associated with Axenfeld-Rieger syndrome (ARS). However, the treatment of patients with ARS remains mostly supportive and palliative.

Methods. The authors used molecular genetic, pharmacologic, and embryologic techniques to study the biology of ARS in a zebrafish model that uses transgenes to mark neural crest and muscle cells in the head.

Results. The authors demonstrated in vivo that *pitx2* is a key downstream target of retinoic acid (RA) in craniofacial development, and this pathway is required for coordinating neural crest, mesoderm, and ocular development. *pitx2a* knockdown using morpholino oligonucleotides disrupts jaw and pharyngeal arch formation and recapitulates ocular characteristics of ARS, including corneal and iris stroma maldevelopment. These phenotypes could be rescued with human *PITX2A* mRNA, demonstrating the specificity of the knockdown and evolutionary conservation of *pitx2a* function. Expression of the ARS dominant negative human *PITX2A* K50E allele also caused ARS-like phenotypes. Similarly, inhibition of RA synthesis in the developing eye (genetic or pharmacologic) disrupted craniofacial and ocular development, and human *PITX2A* mRNA partially rescued these defects.

Conclusions. RA regulation of *pitx2* is essential for coordinating interactions among neural crest, mesoderm, and developing eye. The marked evolutionary conservation of Pitx2 function in eye and craniofacial development makes zebrafish a potentially powerful model of ARS, amenable to in vivo experimentation and development of potential therapies. (*Invest Ophthalmol Vis Sci.* 2012;53:7–22) DOI:10.1167/iovs.11-8494

Axenfeld-Rieger syndrome (ARS, OMIM 180500) is a spectrum of autosomal dominantly inherited malformations that predominantly affect the eye but are also associated with craniofacial dysmorphism and dental abnormalities, including maxillary hypoplasia and microdontia.[1,2] Ocular findings in ARS are typically limited to the anterior segment of the eye and include posterior embryotoxon (anteriorization of the angle structure/Schwalbe's line), iris hypoplasia, and corectopia (maldevelopment of the iris with shifting of the pupil). Secondary glaucoma, caused by iris strands that bridge the iridocorneal angle and trabecular meshwork, can be refractory to treatment and lead to significant visual impairment. Specific gene mutations have been identified in approximately 60% of cases; one of the most commonly affected genes is the paired homeobox transcription factor *PITX2* (see Refs. 3, 4 for review); OMIM 180500). Multiple types of point and chromosomal mutations, which include both gain-of-function and loss-of-function of the *PITX2* gene, have been identified in patients with ARS.[5–9]

The *PITX2* gene codes for as many as four mRNA transcripts (*PITX2*A-D).[10] In humans, *PITX2A*, *B*, *C*, and *D* have been identified, whereas in zebrafish only the *pitx2a* and *pitx2c* isoforms have been detected.[11] *Pitx2* is expressed in cranial neural crest (CNC) and mesoderm-derived cells, which form tissues that interact with the developing eye.[12] The *Pitx2* knockout mouse dies at embryonic day (E) 14.5 because of heart defects and displays severe ocular defects and loss of extraocular muscle (EOM).[13] Conditional knockout studies using mice demonstrated that *Pitx2* in CNC is required for the ocular development and optic stalk formation.[12] In mice, activation of muscle-specific transcription factors in the EOM is dependent on *Pitx2*,[14–16] and *Pitx2* is also required for pharyngeal arch development and subsequent jaw and dental formation.[17–19] Thus, *Pitx2* appears to be critical for craniofacial and ocular development, and the regulation of its expression may mediate interactions among the developing eye, CNC, and mesoderm.

Retinoic acid (RA) is an essential morphogen that regulates craniofacial development in mammals and fish.[20–22] In humans, both the disruption of RA synthesis (e.g., fetal alcohol syndrome) and in utero exposure to excessive retinoids (e.g., through medications such as isotretinoin) can result in craniofacial dysmorphism.[23–26] Studies using mouse models reveal that RA acts as a paracrine signal that is produced by the developing eye and targets the periocular tissues during craniofacial development. Expression of retinaldehyde dehydrogenase (raldh) in the developing eye (retina, lens, and surface ectoderm) is tightly regulated both temporally and spatially.[27,28] An additional gradient is formed through the expres-

From the [1]Department of Ophthalmology and Visual Sciences and the [2]Molecular and Behavioral Neuroscience Institute and Department of Biological Chemistry, University of Michigan, Ann Arbor, Michigan.

Supported by a Research to Prevent Blindness Career Development Award (AK); the Alliance for Vision Research (AK); Postdoctoral Training Grant T32 EY013934 from the National Eye Institute (NEI) of the National Institutes of Health (NIH) (BLB); a Knights Templar Eye Foundation award (BLB); a Fight for Sight student award (DSK); Grants K08 EY018689 (AK) and R01 EY018132 (DG) from the NEI of the NIH; a Vision Research Core Award P30 EY007003 to the Department of Ophthalmology and Visual Sciences, Kellogg Eye Center, University of Michigan; the Zebrafish International Resource Center (supported by Grant P40 RR102546 from the NIH-NCRR); and the Helmut F. Stern Career Development Professorship in Ophthalmology and Visual Sciences (AK).

Submitted for publication August 29, 2011; revised October 9, 2011; accepted November 10, 2011.

Disclosure: **B.L. Bohnsack**, None; **D.S. Kasprick**, None; **P.E. Kish**, None; **D. Goldman**, None; **A. Kahana**, None

Corresponding author: Alon Kahana, 1000 Wall Street, Ann Arbor, MI 48105; akahana@med.umich.edu.

sion of *cyp26*, a cytochrome P450 enzyme, in the central anterior-posterior axis of the retina. This creates an RA-free zone that separates the dorsal from the ventral retina.[29,30] Thus, before the synthesis of visual pigment chromophore in the developing retina, both RA production and degradation are tightly regulated, supporting an early role for RA in ocular and craniofacial development. Indeed, mouse RA receptors RARβ and RARγ are expressed in the periocular mesenchyme and the developing craniofacial region,[31–33] zebrafish *rara* and *rarg* are expressed in the periocular mesenchyme,[34,35] and zebrafish *rara* are also expressed in the EOMs.[36] These studies suggest that RA acts as a paracrine signal with targets in periocular tissues.

Congenital craniofacial abnormalities seen with *pitx2* mutations and alterations in RA levels are caused predominantly by the disruption of neural crest development resulting in anomalies in the underlying bone, cartilage, connective tissue, and eyes. Numerous human disorders, including ARS, have been described as "neurocristopathies".[37] However, there is a wide range in severity of craniofacial defects among these conditions, and the expressivity likely reflects the stage at which the CNC is affected by the underlying genetic or environmental insult. Complex reciprocal interactions between the CNC and the surrounding ectoderm, endoderm, and mesoderm are required for formation of the tissues and the sensory organs of the head.[22,38–44] RA and *pitx2* are two critical regulators of this process, and studies in mouse demonstrate that *Pitx2* is a downstream target of RA in the periocular mesenchyme.[45]

In the present study, an in vivo experimental approach was used to probe the relationship between RA and *PITX2* in ocular and craniofacial development. The results show that RA regulates *pitx2* expression in the periocular mesenchyme and EOMs, and exogenously added human *PITX2* mRNA can compensate for the inhibition of RA synthesis. Furthermore, human *PITX2* mutations associated with ARS,[46–49] and alterations in RA levels or *pitx2* expression, can recapitulate ocular and craniofacial ARS phenotypes in zebrafish. Importantly, human *PITX2* mRNA can rescue the ARS-like phenotypes caused by knockdown of the endogenous zebrafish *pitx2* gene. We conclude that the roles of RA and *PITX2* in ocular and craniofacial development reveal remarkable functional conservation between vertebrate classes. Such conservation can be used to probe the regulation of morphogenesis using a variety of approaches, including in vivo models, and to screen through phenotypic modifiers to identify potential therapies for ARS and other genetic disorders.

Materials and Methods

Zebrafish Care, Mutants, and Transgenics

Zebrafish (*Danio rerio*) were raised in a laboratory breeding colony on a 14-hour light/10-hour dark cycle. Embryos were maintained at 28.5°C and staged as described.[50] Embryo age is defined as hours postfertilization (hpf) or days postfertilization. Tg(*sox10::EGFP*) strain was the generous gift of Thomas Schilling.[51,52] The Tg(*α-actin::EGFP*) strain was a generous gift of Simon Hughes.[53] These transgenic strains were crossed into the Roy background,[54] which was the generous gift of Rachel Wong, to decrease endogenous fluorescence. Phenylthiourea 0.003%, which inhibits pigmentation, was added to the media of embryos harvested for wholemount in situ hybridization.[55] The protocols have met guidelines established by the University of Michigan Committee on the Use and Care of Animals and adhere to the ARVO Statement for the Use of Animals in Ophthalmic and Vision Research.

In Situ Hybridization

In situ hybridization was performed as previously described[56] using digoxigenin (DIG) or fluorescein-labeled RNA antisense probes, or both. RNA probes were in vitro transcribed with T7 or T3 polymerase using PCR product with a 3′ sequence of the appropriate promoter. For colorimetric reactions, probes were labeled with alkaline phosphatase-conjugated antibodies directed against DIG or fluorescein and were visualized with 4-nitroblue tetrazolium/5-bromo-4-chloro-3-indolyl phosphate (NBT/BCIP; Roche Molecular Biochemicals, Indianapolis, IN) or Fast Red (Roche). For fluorescence detection, probe haptens were labeled with peroxidase-conjugated antibodies, and the signal was amplified using tyramide Alexa fluorophores (Invitrogen, Carlsbad, CA) or tyramide Cy fluorophores (Perkin-Elmer, Waltham, MA). Embryos were cryoprotected and embedded in optimum cutting temperature compound for sectioning.

Zebrafish Ocular Histology, Ocular Measurements, and Statistical Analysis

Zebrafish embryos were fixed in 2% paraformaldehyde/1.5% glutaraldehyde overnight at 4°C and then embedded in methyl acrylate. Blocks were sectioned at 5 μm and mounted on slides. Staining with Lee's stain or trichrome-like stain was performed using standard techniques.[57,58] Permanent coverslips were placed using mounting medium (CytoSeal; Richard-Allan Scientific, Kalamazoo, MI). Sections were imaged with an inverted-light microscope (DM6000B; Leica Microsystems CMS GmbH, Wetzlar, Germany) and a color camera (DFC500; Leica Microsystems CMS GmbH). Images were processed using graphics editing software (Photoshop; Adobe Systems, Inc., San Jose, CA) and the Leica LAS application.

Ocular measurements were obtained using ImageJ software (developed by Wayne Rasband, National Institutes of Health, Bethesda, MD; available at http://rsb.info.nih.gov/ij/index.html). For corneal thickness, in each eye a line radial to the central axis of the lens was drawn between the surfaces of the corneal epithelia and the lens epithelia and was measured in microns using three consecutive sections that encompassed the lens equator. The dorsal-ventral dimension of the eye was measured as the distance in microns between the dorsal and ventral retinal pigment epithelia at the equator of the eye in three consecutive sections that encompassed the thickest portion of the lens. The anterior-posterior dimension of the eye was measured as a line perpendicular to the central axis of the lens and was drawn between the surface of the corneal epithelium and the retinal pigment epithelium near the optic stalk in three consecutive sections that encompassed the lens equator. The average of the three consecutive sections for each eye was used for statistical analysis. Six to 10 eyes for each treatment or morpholino/mRNA group were measured.

The Bartlett method was used to determine whether there was equality of SD between the eyes in each group. The Kolmogorov-Smirnov method was used to determine whether the measurements held to a Gaussian distribution. ANOVA with Tukey-Kramer multiple comparisons test was used for comparisons that satisfied the Bartlett and Kolmogorov-Smirnov methods. A Kruskal-Wallis test (nonparametric ANOVA) was used for comparisons that failed the Bartlett or Kolmogorov-Smirnov methods. Statistical significance was considered $P < 0.05$ and specific values are denoted in Tables 1 and 2. All statistical analyses were performed using a statistics program (InStat, version 3; GraphPad, La Jolla, CA).

Oligonucleotide Morpholinos

Antisense oligonucleotide morpholinos (MOs) were synthesized by Gene Tools, LLC (Cowallis, OR) and reconstituted in deionized water. MO sequences for *raldh2*, *p53,* and standard control (*globin*) were previously published.[59,60] MO directed against *raldh3*, *pitx2a,* and *pitx2c* were custom designed according to the manufacturer's specification (sequences in Supplementary Table S1, http://www.iovs.org/lookup/suppl/doi:10.1167/iovs.11-8494/-/DCSupplemental), and the same *raldh3* (*aldh1a3*) morpholino sequence was recently published.[61] The concentration of MO for each gene that yielded consistent and reproducible phenotype was determined. MO sequences that were not lissamine-tagged were coinjected with Texas Red for fluores-

Table 1. Ocular Measurements in 96-hpf Embryos Injected with Oligonucleotide Morpholinos and *PITX2A* mRNA

	Corneal Thickness (μm)	Dorsal-Ventral Dimension (μm)	Anteroposterior Dimension (μm)
(A) Control MO	5.5 ± 0.5	231.4 ± 5.6	171.4 ± 3.7
(B) *pitx2a* MO	7.6 ± 0.7[1*]	158.6 ± 12.4[1*]	145.3 ± 7.4[1*]
(C) *PITX2A* mRNA + control MO	8.2 ± 0.4[1†]	142.2 ± 17.3[1†]	125.7 ± 9.3[1†]
(D) *PITX2A* mRNA + *pitx2a* MO	5.4 ± 0.8[2†,3‡]	246.4 ± 7.6[2†,3†]	170.9 ± 7.0[2†,3†]
(E) K50E *PITX2A* mRNA + control MO	6.1 ± 0.5[3‡]	221.2 ± 4.0[3‡]	165.2 ± 2.9[3‡]
(F) K50E *PITX2A* mRNA + *pitx2a* MO	9.5 ± 2.1[1†,2‡,4†,5†]	171.1 ± 19.9[4*]	167.5 ± 14.6[3‡]
(G) *raldh2/p53* MO	8.6 ± 1.2[1†,4†,5†]	142.9 ± 7.4[1†,4†,5*]	147.9 ± 3.3[1*,4‡]
(H) *PITX2A* mRNA + *raldh2/p53* MO	5.0 ± 1.1[2*,3†,6†,7†]	209.0 ± 10.3	166.4 ± 8.4[3*]
Test used	ANOVA	Kruskal-Wallis	Kruskal-Wallis

Corneal thickness and eye dimensions (dorsal-ventral axis and anteroposterior axis) measured in microns in 96-hpf embryos injected with control MO (A), *pitx2a* MO (B), *PITX2A* mRNA and control MO (C), *PITX2A* and *pitx2a* MO (D), K50E *PITX2A* mRNA + control MO (E), K50E *PITX2A* mRNA + *pitx2a* MO (F), *raldh2/p53* MO (G), or *PITX2A* mRNA + *raldh2/p53* MO (H).

[1]Compared with control MO. [2]Compared with *pitx2a* MO. [3]Compared with *PITX2A* mRNA + control MO. [4]Compared with *PITX2A* mRNA + *pitx2a* MO. [5]Compared with K50E *PITX2A* mRNA + control MO. [6]Compared with K50E *PITX2A* mRNA + *pitx2a* MO. [7]Compared with *raldh2/p53* MO.

* $P < 0.01$; † $P < 0.001$; ‡ $P < 0.05$.

cent tracking; 1 nL MO (0.1–0.5 mM) was injected into the yolk of one- to two-cell–stage embryos.

To test the functionality of the *pitx2a* and *pitx2c* MO (Supplementary Fig. S6, http://www.iovs.org/lookup/suppl/doi:10.1167/iovs.11-8494/-/DCSupplemental), complementary sequences to the MO (sequences in Supplementary Table S1, http://www.iovs.org/lookup/suppl/doi:10.1167/iovs.11-8494/-/DCSupplemental) were cloned, using the Gateway cloning system, into pdEST R4-R3 VECTOR II (final construct: CMV/SP6-*pitx2a/c* complementary sequence of MO-EGFP). mRNA of the complementary sequence was transcribed (mMessage mMachine kit; Ambion Biosystems, Austin, TX), resuspended at 100 to 200 ng/μL in nuclease-free water containing 0.1% phenol red, and injected into embryos with or without the *pitx2a/c* MO at the one-cell stage. Injection of mRNA containing the complementary sequence to the MO resulted in diffuse green fluorescent protein (GFP) expression (Supplementary Figs. S1B, S1G, http://www.iovs.org/lookup/suppl/doi:10.1167/iovs.11-8494/-/DCSupplemental). Coinjection of *pitx2a* or *pitx2c* MO with the corresponding mRNA abrogated GFP expression, demonstrating the specificity of each MO (Supplementary Figs. S1D, S1I, http://www.iovs.org/lookup/suppl/doi:10.1167/iovs.11-8494/-/DCSupplemental). To test the functionality of the raldh3 MO, PCR was used to amplify EGFP from pCS2-EGFP with the raldh3 morpholino binding sequence upstream and in frame with the EGFP start codon using the T3 3′ primer and the following 5′ primer containing the SP6 promoter: 5′- GATTTAGGTGACACTATATGCTATGGCACAGAACGGGACTATAGTGAGCAAGGGCGAGG. After 20 PCR cycles with this primer pair, the product was gel-isolated and used as a template for another PCR cycle using the SP6 and T3 primers. mRNA was synthesized (mMessage mMachine kit; Ambion Biosystems). A control EGFP mRNA was transcribed from a PCR primer pair of SP6 and T3 that lacked the morpholino sequence insert. The MO-EGFP mRNA was coinjected into embryos with either the lissamine-tagged raldh3-MO or an untagged control globin-MO (Supplementary Fig. S2, http://www.iovs.org/lookup/suppl/doi:10.1167/iovs.11-8494/-/DCSupplemental).

Embryos were analyzed with a combi-scope (M205FA; Leica) using bright-field imaging (DFC290; Leica) and fluorescent imaging (ORCA-ER; Hamamatsu, Hamamatsu, Japan) cameras.

mRNA Synthesis and Microinjection

Human *PITX2A* mRNA (wild-type, T30P mutant, K50E mutant) was transcribed from the plasmid pCI vector tagged with HA (generous gifts of Michael Walter and Philip Gage).[62] Capped mRNA was synthesized (mMessage mMachine kit; Ambion Biosystems), and suspended at 100 to 200 ng/μL in nuclease-free water containing 0.05 mM Texas Red. mRNA (1 nL) was injected into one-cell stage embryos.

Pharmacologic Treatment of Embryos

All-*trans* RA (Sigma, St. Louis, MO), diethylbenzaldehyde (DEAB; Sigma), Ro 41–5253 (Enzo Life Sciences, Plymouth Meeting, PA), TTNPB (Ro 13–7410; Enzo Life Sciences), and methoprene acid (GR-106; Enzo Life Sciences) were diluted in dimethyl sulfoxide (DMSO) at 1000× the final concentration. Pharmacologic agents were added to embryo media to their final concentrations (RA, 0.1 nM-1 μM; DEAB, 10–20 μM; Ro 41–52534, 1 μM; TTNPB, 0.01 μM; methoprene acid, 1 μM) at the indicated time. DMSO (0.1%) served as control. Exogenous treatment was initiated at 24 or 28 hpf, as indicated. Embryo media

Table 2. Ocular Measurements in 96-hpf Embryos Treated with Exogenous RA and DEAB

	Corneal Thickness (μm)	Dorsal-Ventral Dimension (μm)	Anteroposterior Dimension (μm)
(A) 0.1% DMSO control	3.6 ± 0.8	231.4 ± 10.1	144.8 ± 10.2
(B) 100 nM RA	7.5 ± 1.0[1*]	184.0 ± 7.2[1*]	134.2 ± 7.5
(C) 10 μM DEAB	8.2 ± 0.8[1*]	195.3 ± 13.2[1*]	156.6 ± 8.3[2‡]
(D) 1 nM RA + 10 μM DEAB	6.7 ± 1.6[1*]	217.6 ± 10.6[1†,2*,3*]	150.5 ± 5.6
(E) 10 nM RA + 10 μM DEAB	4.1 ± 0.8[2*,3*,4*]	214.9 ± 3.5[1†,2*,3‡]	167.3 ± 8.7[2*]
Test used	ANOVA	ANOVA	Kruskal-Wallis

Corneal thickness and eye dimensions (dorsal-ventral axis and anteroposterior axis) measured in microns in 96-hpf embryos treated with 0.1% DMSO (A), 100 nM RA at 28 hpf (B), 10 μM DEAB at 24 hpf (C), 1 nM RA at 28 hpf + 10 μM DEAB at 24 hpf (D), or 10nM RA at 28 hpf + 10 μM DEAB at 24 hpf (E).

[1]Compared with 0.1% DMSO control. [2]Compared with 100 nM RA. [3]Compared with 10 μM DEAB. [4]Compared with 1 nM RA + 10 μM DEAB.

* $P < 0.001$; † $P < 0.05$; ‡ $P < 0.01$.

were changed every 24 hours with fresh pharmacologic agent until the embryos were harvested.

Zebrafish Enucleation and Bead Experiments

AG 1-X8 ion-exchange beads (40–60 μm) were soaked in DMSO or 100 nM RA diluted in DMSO for 1 hour before implantation.[63] Embryos from Tg(*sox10::EGFP*) and Tg(*α-actin::EGFP*) zebrafish were dechorionated and enucleated at 16 hpf using sharp tungsten needles and a dissecting microscope. Care was taken not to injure the cranium or the surrounding orbit during the procedure. A DMSO- or RA-soaked bead was placed in the orbit. The embryos were then returned to zebrafish growth medium and allowed to recover at 28.5°C. Embryos were imaged at 72 and 96 hpf and harvested in 4% paraformaldehyde.

Results

Pitx2a Is Required for Ocular Development in Zebrafish Embryos

Given that haploinsufficiency of *PITX2* in humans and mice results in the dysgenesis of the anterior segment of the eye,[3,4,49,64–66] we first determined whether these findings could be recapitulated in zebrafish by injecting MO targeting *pitx2a* at the one- to two-cell stage (Figs. 1A–E). Indeed at 96 hpf, relative to controls, MO knockdown of *pitx2a* resulted in maldeveloped eyes that were significantly smaller in the dorsal-ventral ($P < 0.01$) and anterior-posterior ($P < 0.01$) axes (Table 1; compare Figs. 1A and 1P). The corneas in *pitx2a* MO knockdown embryos were significantly thicker ($P < 0.01$; Table 1, compare Figs. 1G and 1Q). The corneal epithelium in *pitx2a* MO knockdown embryos was disorganized and had a scalloped appearance, more similar to skin than to the smooth surface observed in control corneas. Using a trichrome-like stain, which better highlighted the corneal layers, it was evident that *pitx2a* MO embryos lacked a definitive corneal endothelium (compare Figs. 1G and 1Q). By 96 hpf, the dorsal iridocorneal angle of the control MO embryos contained CNC-derived iris stromal cells, including xanthophores, iridophores, and undifferentiated cells (Fig. 1R). The ventral iridocorneal angle, which has been previously described to be less cellular and slightly developmentally delayed compared with the dorsal angle,[67] contained numerous undifferentiated cells in the control embryos (data not shown). After *pitx2a* knockdown, there was decreased cellularity in the dorsal (Fig. 1C) and ventral (data not shown) iridocorneal angles. Retinas in *pitx2a* MO lacked photoreceptor outer segments (Fig. 1E) but were otherwise similar to control (Fig. 1L). Thus, the knockdown of *pitx2a* expression in zebrafish embryos recapitulates features of the ocular phenotype in ARS.

Because both loss-of function and gain-of-function mutations are associated with ARS, we took advantage of the accessibility of zebrafish embryos and investigated whether microinjection of human *PITX2A* mRNA into one-cell stage embryos also disrupted ocular development. Injection of 1 nL of 75 ng/μL wild-type human *PITX2A* mRNA along with control MO resulted in eyes with thickened corneas ($P < 0.001$; Table 1, Fig. 1G). As observed in the *pitx2a* MO knockdown, the epithelium had a scalloped surface and the corneas lacked endothelium in embryos injected with human *PITX2A* mRNA and control MO. Dorsal (Fig. 1H) and ventral iridocorneal angles of the embryos injected with human *PITX2A* mRNA also had decreased cellular structure compared with control (Fig. 1R). In contrast to the MO knockdown, the retinas of embryos injected with human *PITX2A* mRNA appeared normal (Fig. 1J).

We next determined whether the human allele of *PITX2A* mRNA could substitute for the zebrafish homolog and rescue the ocular phenotype in the zebrafish *pitx2a* MO knockdown. Coinjection of human *PITX2A* mRNA with the *pitx2a* MO completely restored ocular morphology (Fig. 1K), including the dimensions of the eye (Table 1), corneal architecture (Fig. 1L), angle structure (Fig. 1M), and retinal formation (Fig. 1O). Thus, there is functional homology between human and zebrafish forms of *pitx2a* in ocular development.

The K50E mutation (with a substitution of lysine for glutamate) in *PITX2A*, which was identified in ARS patients, alters the conserved lysine in the DNA-binding domain, leading to a dominant negative effect by sequestration of cofactors and preventing wild-type *PITX2A* protein from activating target gene transcription.[8,46] We synthesized human *PITX2A* mRNA containing the K50E mutation and microinjected the mRNA (1 nL of 75 ng/μL) along with control MO or the *pitx2a* MO into zebrafish embryos at the one-cell stage. Expression of the dominant negative K50E human *PITX2A*, when coinjected with control MO, did not significantly alter ocular size, anterior segment formation, or retinal development (Supplementary Figs. S3A–E, http://www.iovs.org/lookup/suppl/doi:10.1167/iovs.11-8494/-/DCSupplemental) compared with embryos injected with control MO alone. On the other hand, expression of K50E human *PITX2A*, together with morpholino knockdown of the zebrafish *pitx2a* (Supplementary Fig. S3F–J, http://www.iovs.org/lookup/suppl/doi:10.1167/iovs.11-8494/-/DCSupplemental), resulted in an additive phenotype, worse than *pitx2a* knockdown alone (Figs. 1A–E). In these embryos (Table 1) the corneas were significantly ($P < 0.001$) thickened (Table 1; Supplementary Fig. S3G, http://www.iovs.org/lookup/suppl/doi:10.1167/iovs.11-8494/-/DCSupplemental) and lacked endothelium, whereas the dorsal (Supplementary Fig. S3H, http://www.iovs.org/lookup/suppl/doi:10.1167/iovs.11-8494/-/DCSupplemental) and ventral (data not shown) iridocorneal angles were almost devoid of iris stromal cells. The retinas were disorganized and showed loss of cells (Supplementary Fig. S3J, http://www.iovs.org/lookup/suppl/doi:10.1167/iovs.11-8494/-/DCSupplemental).

Pitx2a Regulates CNC in Craniofacial Development in Zebrafish Embryos

Because ARS can be associated with craniofacial dysmorphism and *Pitx2* mutations in mice cause pharyngeal arch and EOM defects,[14,15,18,19] we next used an in vivo approach to investigate the role of *pitx2* on CNC and muscle development using transgenic fish in which GFP is expressed in neural crest cells or differentiated muscle [Tg(*sox10::EGFP*) or Tg(*α-actin::EGFP*)].[51–53,68,69] Knockdown of the *pitx2a* isoform in Tg(*sox10::EGFP*) embryos demonstrated that at 72 hpf (data not shown) and 96 hpf, CNC-derived jaw cartilage was maldeveloped and the pharyngeal arch cartilage was absent (compare Figs. 2A and 2B). Similarly, knockdown of *pitx2a* in Tg(*α-actin::EGFP*) embryos resulted in abnormal jaw musculature and no pharyngeal arch musculature (compare Figs. 3A and 2B; compare Figs. 1A and 1P). In addition, knockdown of *pitx2a* was associated with EOM insertions that were placed closer together because of the smaller eye size (Fig. 3A). Cross-sections of the medial rectus in the *pitx2a* knockdown embryos (Fig. 1D) demonstrated disorganization of myofibers and thickening of the muscle. Knockdown of the *pitx2c* isoform, in contrast to *pitx2a,* showed no discernible craniofacial phenotypes (data not shown), consistent with the different roles of these isoforms in embryogenesis.[70,71]

Given the functional equivalence of human *PITX2A* in ocular development, we tested the effect of injecting wild-type human *PITX2A* mRNA on CNC and muscle development. Overexpression of human *PITX2A* revealed malformation of jaw and pharyngeal arch cartilage (Fig. 2D) and minimal changes in jaw, pharyngeal arch, and EOM formation (Fig. 3D; see also Figs. 1F, 1I).

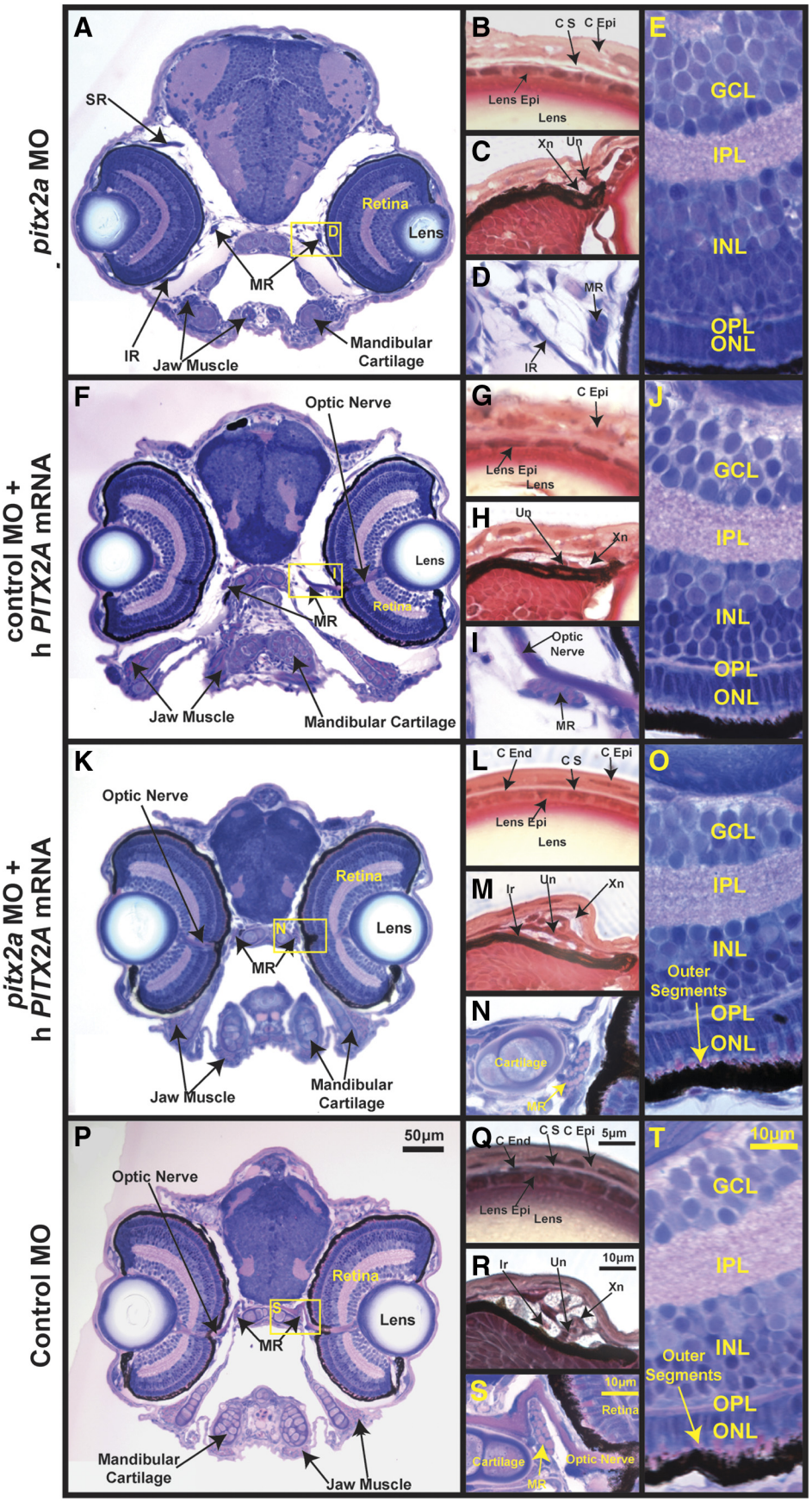

Figure 1. *Pitx2* regulates zebrafish ocular development. Embryos that were injected at the one-cell stage with antisense oligonucleotide MO directed against *pitx2a* MO (**A**–**E**), human wild-type *PITX2A* mRNA with control MO (**F**–**J**), human wild-type *PITX2A* mRNA with *pitx2a* MO (**K**–**O**), or control MO (**P**–**T**) were harvested at 96 hpf. Coronal plastic sections demonstrated that *pitx2a* MO knockdown resulted in small eyes and malformed jaw cartilage and muscles (**A**) compared with control embryos (**P**). Trichrome-like stain demonstrated thickened corneas with a scalloped epithelial (C Epi) surface and a lack of endothelial cells in *pitx2a* MO knockdown embryos (**B**) compared with the corneas in control embryos (**Q**). The dorsal iridocorneal angle of the *pitx2a* MO knockdown embryos (**C**) had fewer iris stromal cells, including Xn, Ir, and Un, which are seen in the control MO (**R**). The medial rectus (MR) in *pitx2a* MO knockdown on cross-section was thickened and contained disorganized myofibers (**D**) compared with the MR in the control MO (**S**). The developing retina in *pitx2a* MO knockdown embryos (**E**) showed mild disorganization of the inner nuclear layer (INL), poor demarcation of the outer plexiform layer (OPL), and lack of photoreceptor outer segment. Coinjection of human *PITX2A* mRNA with control MO similarly resulted in thickened corneas (**G**) with a scalloped appearance that lacked endothelial cells and dorsal iridocorneal angles (**H**) that contained fewer iris stromal cells. Injection of human *PITX2A* mRNA with control MO did not disrupt proper medial rectus formation (**I**) or retinal (**J**) development. Coinjection of human *PITX2A* mRNA with *pitx2a* MO restored corneal architecture (**L**), dorsal iridocorneal angle cellularity (**M**), myofiber organization in the medial rectus (**N**), and retinal development (**O**). SR, superior rectus; IR, inferior rectus; MR, medial rectus; C Epi, corneal epithelium; C S, corneal stroma; C End, corneal endothelium; Lens Epi, lens epithelium; Xn, xanthophore; Ir, iridophore; Un, undifferentiated cell; GCL, ganglion cell layer; IPL, inner plexiform layer; INL, inner nuclear layer; OPL, outer plexiform layer; ONL, outer nuclear layer.

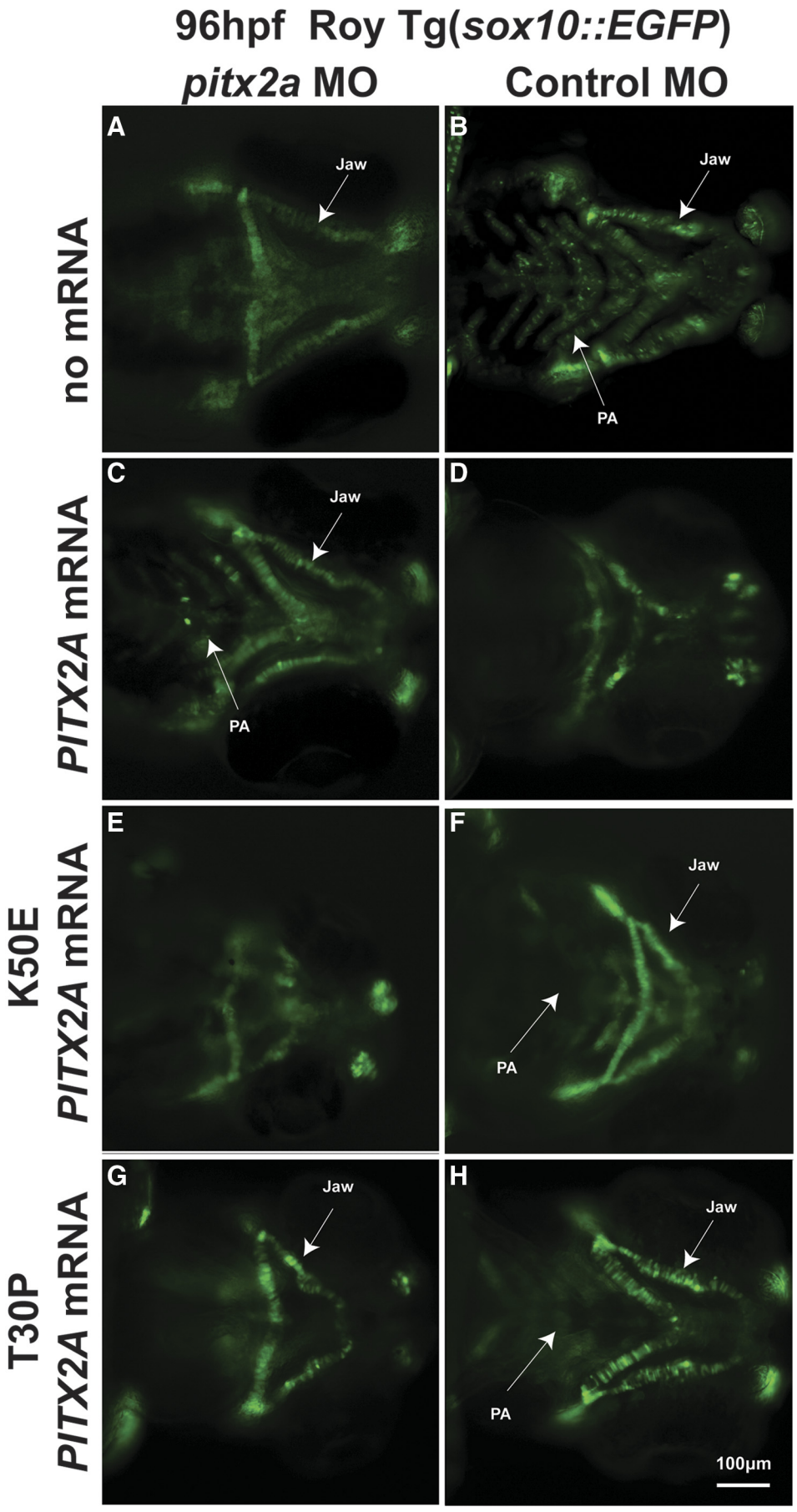

Figure 2. *pitx2* is required for zebrafish CNC development. Microinjection of MO directed against *pitx2a* (**A**) at the one- to two-cell stage into Tg(*sox10::EGFP*) embryos demonstrated at 96 hpf inhibition of neural crest-derived PA development and jaw malformation compared with control MO embryos (**B**). Coinjection of human *PITX2A* mRNA with *pitx2a* MO partially rescued jaw cartilage and PA formation (**C**), whereas injection of human *PITX2A* mRNA with control MO also suppressed PA and jaw development (**D**). Injection of the human dominant negative K50E mutant allele of *PITX2A* resulted in deformed jaw and PA formation when coinjected with control MO (**F**) and complete jaw and PA suppression when coinjected with *pitx2a* MO (**E**). Human *PITX2A* mRNA from the T30P autosomal recessive allele did not affect PA or jaw development when coinjected with control MO (**H**), nor did it rescue the defects when coinjected with *pitx2a* MO (**G**). PA, pharyngeal arch.

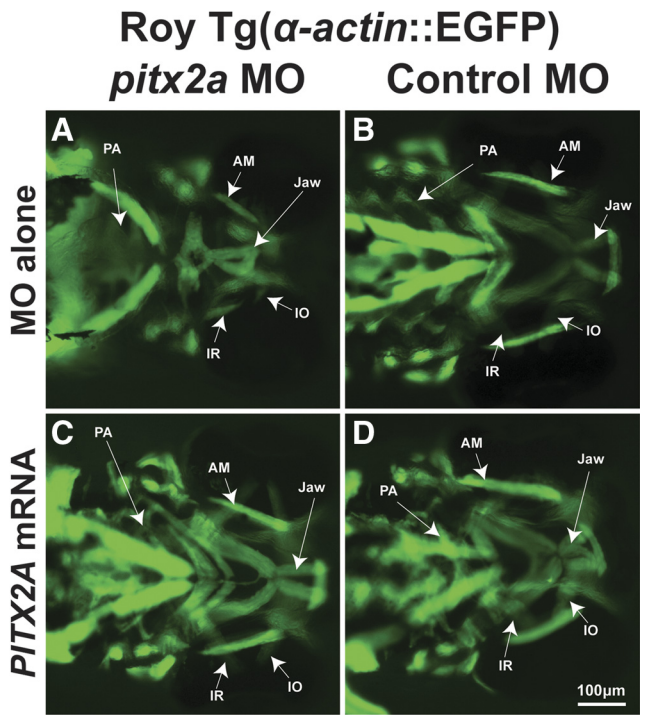

FIGURE 3. *pitx2a* regulates craniofacial muscle development in zebrafish. Tg(*α-actin::EGFP*) embryos that were injected with *pitx2a* MO at the one- to two-cell stage demonstrated malformed PA and jaw muscle formation at 96 hpf (**A**) compared with control embryos (**B**). MO knockdown of *pitx2a* did not affect EOM organization. Coinjection of human *PITX2A* mRNA with *pitx2a* MO restored jaw and PA muscle development (**C**). Injection of human *PITX2A* mRNA with control MO caused mild deformities of jaw and PA musculature (**D**). PA, pharyngeal arch.

Because the wild-type human *PITX2A* mRNA was able to substitute for the zebrafish homolog in ocular development, we next tested whether this was also true for CNC and craniofacial muscle development. Coinjection of *pitx2a* MO and human *PITX2A* mRNA resulted in restoration of jaw cartilage and muscle morphology and partial rescue of pharyngeal arch cartilage and muscle formation (Figs. 2C, 3C) compared with injection of *pitx2a* MO alone (Figs. 2A, 3A).

Although injection of K50E mutant *PITX2A* mRNA had minimal effect on ocular development, we examined the effect of this dominant negative mutant on jaw and pharyngeal arch formation. Injection of K50E mutant human *PITX2A* mRNA resulted in malformed jaw cartilage and inhibition of pharyngeal arch formation (Fig. 2F). Coinjection of K50E mutant human *PITX2A* mRNA with *pitx2a* MO resulted in a more severe phenotype (Fig. 2E) than either the mutant mRNA (Fig. 2F) or *pitx2a* MO (Fig. 2A) alone.

We next tested another ARS-related mutation in the *PITX2* gene, the recessive T30P mutant (substituting threonine for proline).[48,49] Unlike the K50E mutant, T30P does not prevent wild-type *PITX2* from activating gene transcription, although it is transactivation defective.[48,49,72,73] Microinjection of T30P mutant *PITX2A* mRNA may have a very mild effect on jaw or pharyngeal arch cartilage formation (Fig. 2H) at 96 hpf. Furthermore, injection of T30P mutant *PITX2A* mRNA did not rescue the jaw and pharyngeal arch defects caused by *pitx2a* knockdown (Fig. 2G).

Taken together, these results demonstrate that in addition to ocular morphogenesis, *pitx2* is required for the formation of CNC and mesoderm-derived structures in craniofacial development. Furthermore, these data demonstrate a remarkable level of functional conservation of *pitx2* activity between fish and humans.

Pitx2a Expression Is Regulated by RA in the Perioptic Mesenchyme and Developing Jaw

In mice, *pitx2* expression in the perioptic mesenchyme is regulated by RA.[45] We investigated whether this was also true in zebrafish. Colorimetric and fluorescent in situ hybridization of *pitx2* between 24 hpf and 72 hpf revealed expression in the periocular mesenchyme, developing jaw, and brain (Figs. 4C, 4F; Supplementary Figs. S4C, S4F, S4I, http://www.iovs.org/lookup/suppl/doi:10.1167/iovs.11-8494/-/DCSupplemental, [48 hpf]; data not shown). Furthermore, *pitx2* was colocalized with the muscle-specific transcription factor *myoD* by double in situ hybridization, demonstrating the expression of *pitx2* in the mesoderm, which gives rise to the EOM (Fig. 4G).

We next determined whether alterations in RA levels affected *pitx2* expression. RA signaling is known to regulate early developmental processes such as gastrulation, axis formation, and neural crest specification and migration. To avoid confounding effects from these earlier processes,[74,75] we added exogenous all-*trans* RA or the pan-aldehyde dehydrogenase inhibitor diethylbenzaldehyde (DEAB, which inhibits RA synthesis) to the embryo media at 28 hpf or 24 hpf, respectively. Treatment with RA (1–2 μM; Figs. 4A, 4D; Supplementary Figs. S4A, S4D, S4G, http://www.iovs.org/lookup/suppl/doi:10.1167/iovs.11-8494/-/DCSupplemental), upregulated *pitx2* expression in the periocular mesenchyme and jaw. In contrast, exogenous RA decreased the expression of *pitx2* in the brain. Inhibition of RA synthesis by treatment with DEAB (10–20 μM; Figs. 4B, 4E; Supplementary Figs. S4B, S4E, S4H, http://www.iovs.org/lookup/suppl/doi:10.1167/iovs.11-8494/-/DCSupplemental) starting at 24 hpf decreased *pitx2* expression in the periocular mesenchyme but appeared to increase expression in the brain. Thus, RA is a positive regulator of *pitx2* expression in the periocular mesenchyme and jaw and a negative regulator of *pitx2* expression in the brain, revealing the complexity of this regulatory cascade.

RA Regulates Ocular Development

The regulation of *pitx2* by RA led us to investigate whether exogenous treatment with RA or DEAB had effects similar to those of alterations in *pitx2* expression on ocular and craniofacial development. Embryos were treated with exogenous RA or DEAB starting at 28 or 24 hpf, respectively, and then ocular development was examined at 96 hpf. Similar to knockdown of *pitx2a* expression, we found that treatment with exogenous RA (100 nM; Fig. 5A) starting at 28 hpf resulted in eyes with thickened corneas ($P < 0.001$) that were significantly smaller in the dorsal-ventral ($P < 0.001$) and anterior-posterior ($P < 0.01$) axes (Table 2) at 96 hpf. RA treatment impaired anterior segment development because there was no defined corneal endothelium (Fig. 5B) and there were fewer cells in the dorsal (Fig. 5C) and ventral (data not shown) iridocorneal angles. This was in contrast to DMSO-treated control embryos (Fig. 5K) in which the eyes showed well-defined corneal endothelia (Fig. 5L) and dorsal iridocorneal angles that contained iridophores, xanthophores, and undifferentiated cells (Fig. 5M). The inner nuclear layer of the retina in RA-treated embryos was also mildly disorganized, and the photoreceptor outer segment failed to form (Fig. 5E). These features have some overlap with the *pitx2a* knockdown ocular phenotypes.

Inhibition of RA synthesis with DEAB also caused ocular maldevelopment. The eyes of embryos treated with 10 μM DEAB from 24 to 96 hpf (Fig. 5F, Table 2) were mildly but significantly ($P < 0.001$) smaller in the dorsal-ventral axis than they were in controls (Fig. 5K, Table 2). The corneas of DEAB-treated embryos, which were significantly thickened ($P <$

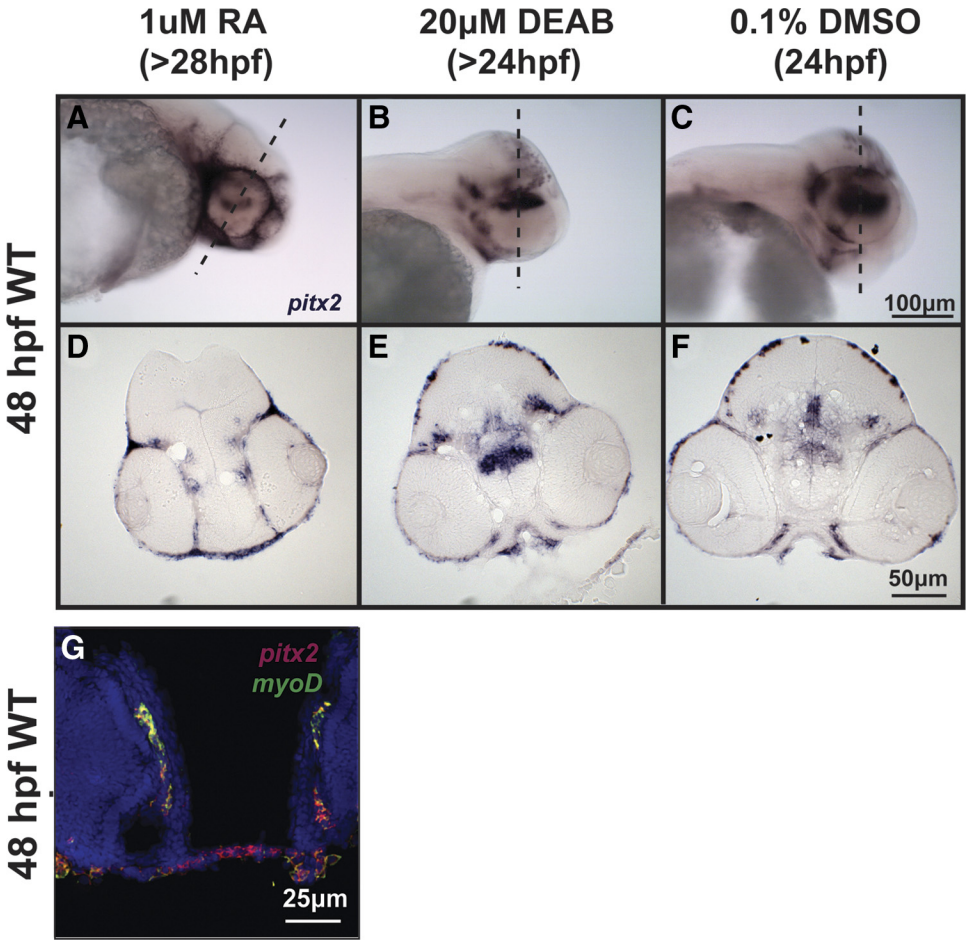

Figure 4. *pitx2* expression in the periocular mesenchyme of the developing zebrafish is regulated by RA. Whole mount and section colorimetric in situ hybridization of 48 hpf wild-type embryos revealed expression of *pitx2* in the periocular mesenchyme, developing jaw, PA, and pituitary in DMSO-treated embryos (**C**, **F**). Treatment of embryos with 1 μM RA, starting at 28 hpf, increased *pitx2* expression in the orbit and jaw but decreased *pitx2* expression in the developing pituitary (**A**, **D**). *pitx2* expression was decreased throughout the periocular mesenchyme but increased in the pituitary with treatment with 20 μM DEAB at 24 hpf (**B**, **E**). Double fluorescent in situ hybridization (**G**) demonstrated colocalization of *pitx2* (*pink*) expression in the periocular mesenchyme with the muscle-specific transcript *myoD* (*green*) in 48 hpf wild-type embryos.

0.001; Table 2), had a scalloped epithelium but contained a defined endothelial layer (Fig. 5G). The dorsal (Fig. 5H) and ventral (data not shown) iridocorneal angles in DEAB-treated embryos were less cellular than in controls (Fig. 5M). As in the *pitx2a* knockdown embryos, the retinas in DEAB-treated embryos also showed ill-defined outer plexiform layer and lack of outer segment (Fig. 5J). Hence, inhibiting RA synthesis also recapitulates many of the *pitx2a* knockdown phenotypes.

Given that both reduced and excess RA levels can induce eye defects, we tested whether exogenous RA can compensate for the inhibition of RA synthesis by DEAB. After treatment with 10 μM DEAB at 24 hpf, RA (1 nM or 10 nM) was added to the embryo media at 28 hpf. We found that 1 nM RA improved, but did not restore, the DEAB effect on corneal thickness and ocular size (Table 2). Treatment with 10 nM RA also improved the DEAB effect on ocular size and restored corneal architecture and thickness (Table 2), anterior segment formation, and retinal development (data not shown).

Taken together, these data demonstrate that regulation of RA levels during the pharyngula, hatching, and early larval stages[50] is required for proper ocular development, including eye size, anterior segment formation, and retinal development. Furthermore, the embryo is very sensitive to alterations in RA levels.

Craniofacial Tissues Have Different Sensitivities to RA

Because deficiencies and overexposure to RA can lead to craniofacial anomalies, we next investigated the effects of exogenous treatment with RA or DEAB on craniofacial development. Increasing concentrations of RA (0.1 nM-1 μM) starting at 28 hpf disrupted CNC development, and 100 nM completely inhibited pharyngeal arch and jaw formation (Figs. 6A, 6D). RA at concentrations higher than 100 nM caused marked growth and developmental arrest and death by 72 hpf (data not shown). In contrast, 96 hpf control embryos had cartilage that demarcated five to six well-developed pharyngeal arches and a protruding jaw (Fig. 6C, 6F). Similarly, embryos treated with 100 nM RA starting at 28 hpf developed only primitive jaw musculature, and there was a complete lack of pharyngeal arch muscles and EOMs (Figs. 6G, 6J, see also Figs. 5A, 5D). Inhibition of RA synthesis by treatment with 10 μM DEAB starting at 24 hpf resulted in only two distinct pharyngeal arches and a jaw that was shortened and malformed (Figs. 6B, 6E, 6H). However, treatment with 10 μM DEAB largely did not affect the differentiation and organization of the EOMs (Fig. 6K), and the medial rectus showed relatively normal appearance of myofibers (Fig. 5I).

Based on our findings that both reduced and excessive RA levels caused dysregulated craniofacial development, we tested whether exogenous RA could rescue pharmacologic inhibition of raldh. After treatment with DEAB at 24 hpf, the addition of different concentrations of exogenous RA (0.1 nM, 1 nM, 10 nM, 100 nM) at 28 hpf rescued craniofacial development by 96 hpf. However, the pharyngeal arches, jaws, and EOMs had different sensitivities to RA. After treatment with 10 μM DEAB, lower concentrations of exogenous RA (0.1–1 nM) improved jaw cartilage and muscle formation (Figs. 7C, 7D, 7K, 7L), whereas higher concentrations of RA disrupted jaw formation (Figs. 7A, 7B, 7I, 7J). In contrast, formation of the five pharyngeal arches occurred only with 10 nM RA (Figs. 7F, 7J). Lower concentrations of RA (Figs. 7G, 7H, 7K, 7L) did not abrogate the DEAB effect on the

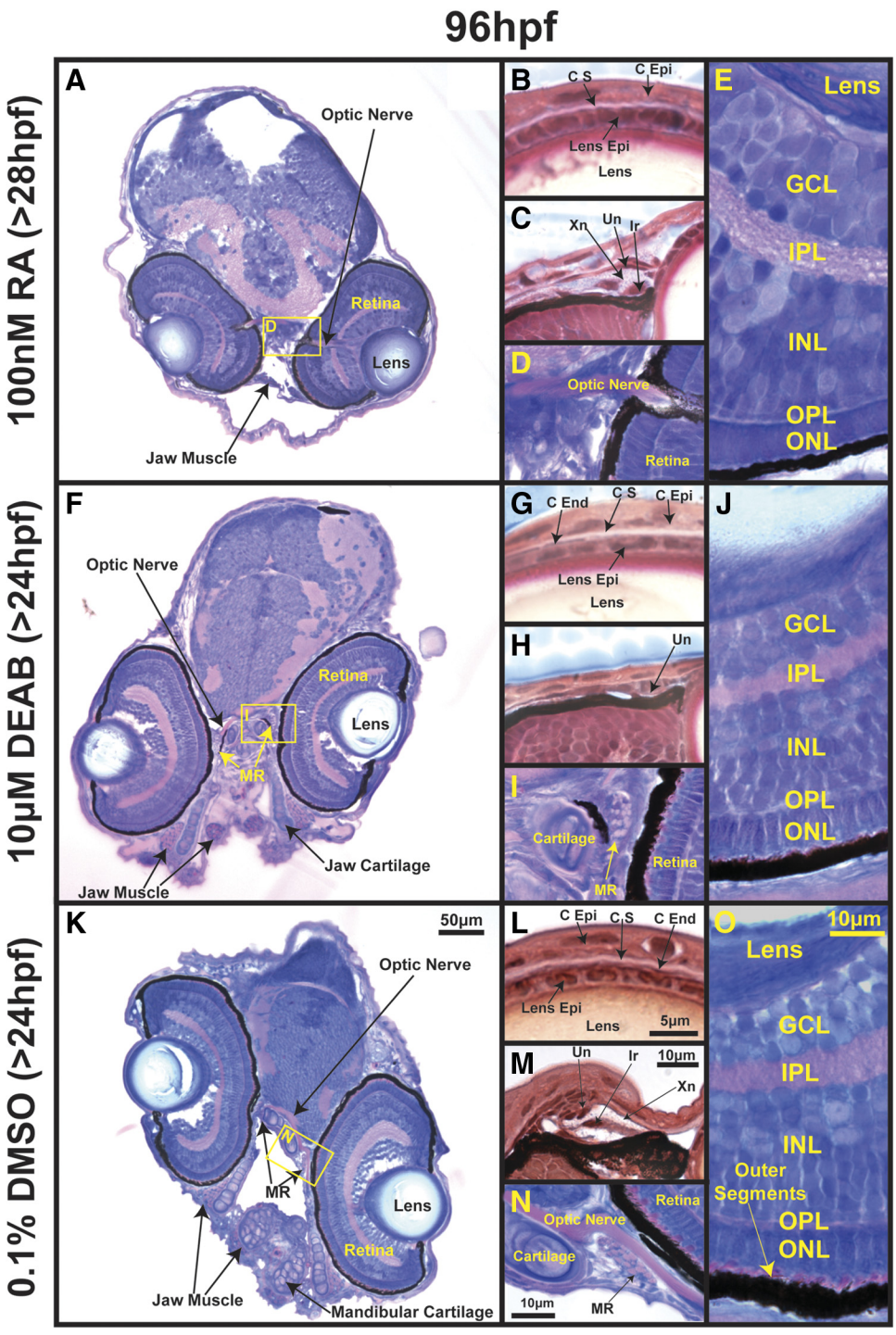

FIGURE 5. Excessive RA and pharmacologic inhibition of RA synthesis alter ocular development in zebrafish. Coronal plastic sections of 96-hpf embryos treated with 100 nm RA (**A**–**E**) starting at 28 hpf demonstrated smaller, malformed eyes and complete lack of jaw formation (**A**) compared with 0.1% DMSO control (**K**). Trichrome-like stain of RA-treated embryos demonstrated lack of corneal endothelial cells (**B**) and decreased iris stromal cells in the dorsal iridocorneal angle (**C**) compared with DMSO-control treated embryos (**L**, **M**). High magnification of the medial orbit in RA-treated embryos (**D**) revealed no identifiable MR compared with a cross-section in control embryos (**N**). The developing retina in RA-treated embryos (**E**) demonstrated disorganization of the INL, poor demarcation of the OPL, and lack of photoreceptor outer segment formation compared with control embryos (**O**). Treatment with the pan-aldehyde dehydrogenase inhibitor DEAB (10 μM) starting at 24 hpf resulted in smaller eyes and mild disruption of jaw cartilage and muscle formation (**F**) compared with DMSO control (**K**). Trichrome-like stain of corneas of embryos treated with DEAB revealed a mildly thickened and scalloped epithelial (**G**, C Epi) surface but maintenance of stromal and endothelial layers. The dorsal iridocorneal angle of DEAB-treated embryos (**H**) had decreased differentiated and undifferentiated iris stromal cells compared with DMSO control (**M**). The MR in DEAB-treated embryos (**I**) in cross-section was mildly thickened compared with DMSO control (**N**). The retina in DEAB-treated embryos (**J**) demonstrated mild disorganization of the INL, poor demarcation of the OPL, and lack of photoreceptor outer segment formation compared with control embryos (**O**). MR, medial rectus; C Epi, corneal epithelium; C S, corneal stroma; C End, corneal endothelium; Lens Epi, lens epithelium; Xn, xanthophore; Ir, iridophore; Un, undifferentiated cell; GCL, ganglion cell layer; IPL, inner plexiform layer; INL, inner nuclear layer; OPL, outer plexiform layer; ONL, outer nuclear layer.

pharyngeal arches, whereas higher concentrations (Figs. 7E, 7I) had a teratogenic effect. EOMs were the least sensitive to alterations in RA because treatment with DEAB alone or with RA concentrations up to 1 nM (Figs. 7O, 7P) had minimal effect on EOM organization. Interestingly, treatment with 10 nM RA and 10 μM DEAB resulted in inferior oblique and rectus muscles that were attached to each other at the midline (Fig. 7N).

To determine whether the effects of exogenous RA or DEAB occurred through the activation of RARs, we tested whether treatment with RAR agonists or antagonists affected craniofacial development. Treatment with Ro 41–5253, a selective RARα antagonist at 24 hpf, recapitulated the effects of DEAB-mediated inhibition of RA synthesis (data not shown). Furthermore, treatment at 24 hpf with TTNPB (Ro 13–7410), a selective RAR agonist, mimicked the effects of exogenous RA. In contrast, treatment at 24 hpf with methoprene acid, an RXR agonist, did not alter CNC and EOM development (data not shown). Thus, in zebrafish the effects of RA on craniofacial formation are mediated by RAR.

RA Is Produced by the Developing Eye during Zebrafish Embryogenesis

The effect of pharmacologic alterations in RA levels on ocular and craniofacial development after early events during embryogenesis led us to further investigate the source of RA produc-

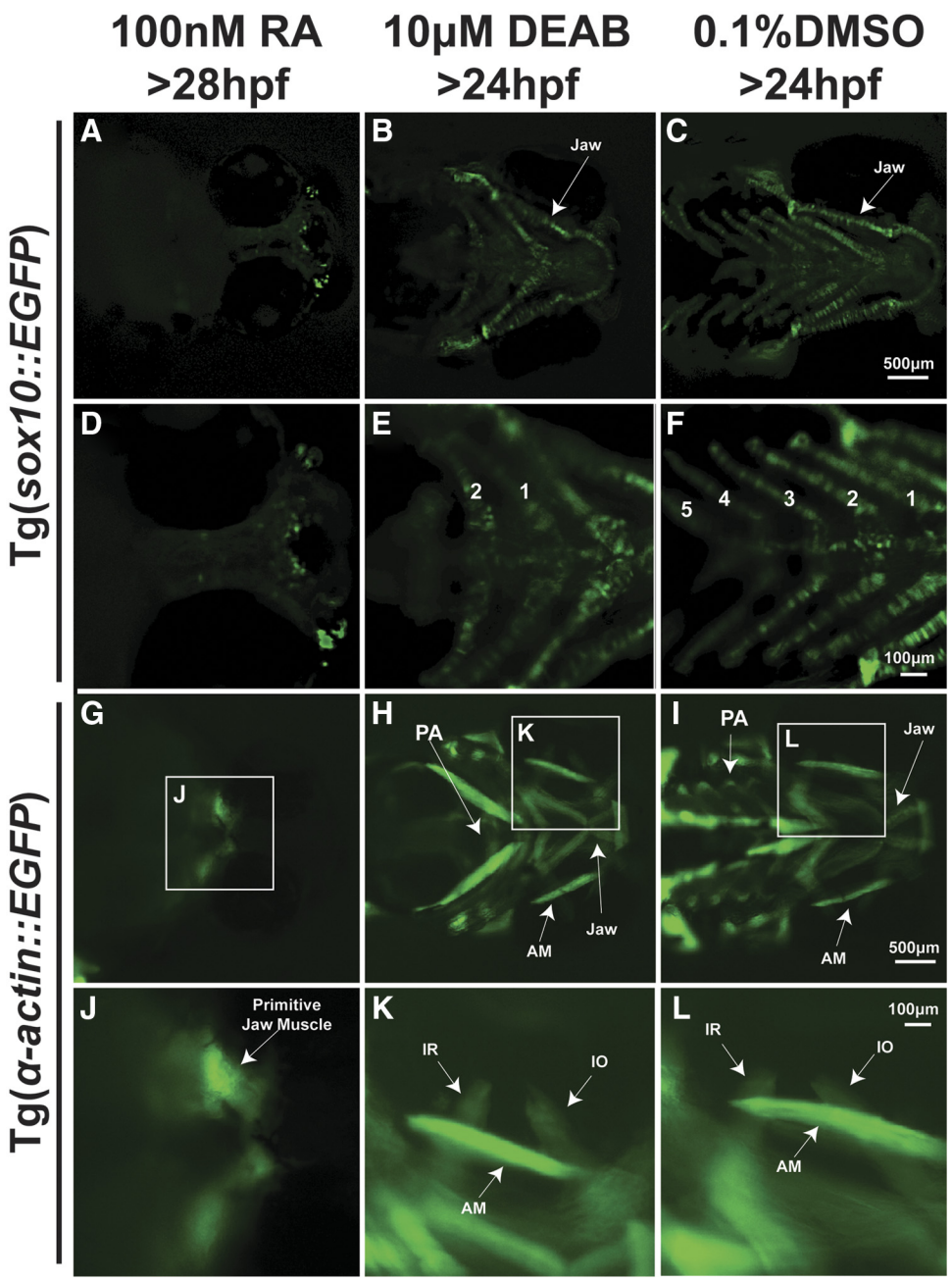

Figure 6. Excessive RA and pharmacologic inhibition of RA synthesis disrupt zebrafish craniofacial development. Tg(*sox10::EGFP*) embryos (**A–F**) treated with 100 nM RA starting at 28 hpf showed an almost complete lack of neural crest with no formation of PA or jaw (**A**, **D**). In Tg(*α-actin::EGFP*) embryos, 100 nM RA treatment showed absence of PA and extraocular musculature and only formation of primitive jaw muscle (**G**, **J**) compared with control DMSO-treated embryos (**I**, **L**). Tg(*sox10::EGFP*) and Tg(*α-actin::EGFP*) embryos treated with 10 μM DEAB starting at 24 hpf had mildly malformed jaws (**B**, **H**) and only two PAs (**E**, **H**) compared with the protruding jaws (**C**, **I**) and five to six well-developed PAs (**F**, **I**) seen in control DMSO-treated embryos. DEAB treatment alone (**K**) did not have an effect on EOM organization when compared with control DMSO (**L**). PA, pharyngeal arch; IR, inferior rectus; IO, inferior oblique; AM, anterior mandibulae.

tion in zebrafish embryos. In situ hybridization in 36-hpf zebrafish embryos demonstrated that *raldh2* was expressed predominantly in the anterodorsal retina (Figs. 8A, 8B), whereas *raldh3* was expressed in the posteroventral retina (Figs. 8A, 8B). Raldh2 expression was also noted in the brain ventricle, but no other adjacent RA source was noted at this stage of development.

Knockdown of *raldh2*, but Not *raldh3,* Disrupts Ocular and Craniofacial Development

We further investigated the role of RA on ocular and craniofacial development by using MO directed against *raldh2* and *raldh3.* Injection of *raldh2* MO into one- to two-cell stage embryos recapitulated the previously described[59] *neckless* phenotype, which characteristically has anteroposterior axis truncation anterior to the somites, absence of pectoral fins, and midline defects. Similar results were obtained when we combine MO knockdown of *raldh2* with MO knockdown of *p53* to reduce apoptosis and nonspecific phenotypes. Knockdown of *raldh2* and *p53* resulted in maldeveloped eyes (Table 1, Fig. 8C) that were similar in appearance to those observed in the *pitx2a* knockdown embryos (Fig. 1A). These embryos had smaller malformed lenses that contained areas devoid of lens fibers (Figs. 8C, 8E asterisks). Corneas in *raldh2/p53* MO knockdown embryos (Fig. 8D) were significantly thicker than in control ($P < 0.001$; Table 1) and had a scalloped epithelium and no endothelium. There was decreased cellularity in the dorsal (compare Figs. 8E and 1R) and ventral (data not shown) iridocorneal angles, and the retinas were mildly disorganized with an ill-defined outer plexiform layer and a lack of photoreceptor outer segment (Fig. 8G).

We next used an in vivo approach to test the effects of *raldh2* knockdown on craniofacial cartilage and muscle

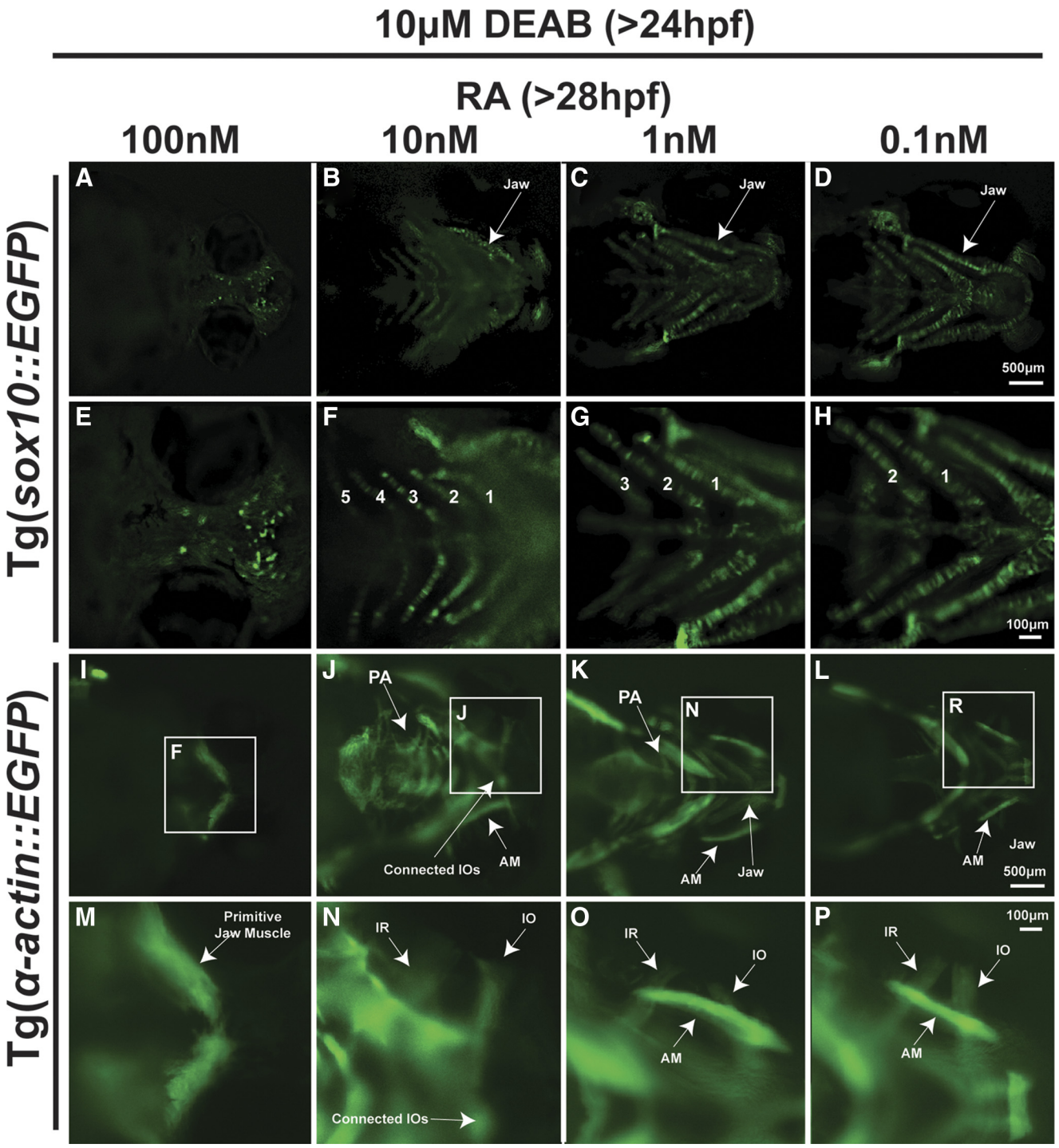

Figure 7. Zebrafish craniofacial structures have different sensitivities to RA. After treatment with 10 μM DEAB at 24 hpf, Tg(*sox10::EGFP*) (**A**–**H**) or Tg(*α-actin::EGFP*) (**I**–**P**) embryos were treated with increasing concentrations of RA (0.1–100 nM) at 28 hpf. Treatment with 0.1 nM and 1 nM RA rescued the DEAB-induced jaw cartilage (**C**, **D**) and muscle (**K**, **L**) defects but did not rescue PA structure (**G**, **H**, **K**, **L**). Treatment with 10 nM RA restored five PAs (**F**) but disrupted jaw cartilage (**B**) and muscle (**J**) development. Treatment with 100 nM RA with 10 μM DEAB inhibited jaw and PA cartilage (**A**, **E**) and muscle (**I**, **M**) development. After treatment with 10 μM DEAB, treatment with 0.1 nM and 1 nM RA did not affect EOM organization (**O**, **P**). Treatment with 10 nM RA with 10 μM DEAB resulted in EOMs that were thickened and disorganized as the IO muscles were connected to each other. IO, inferior oblique; PA, pharyngeal arch.

development. Knockdown of *raldh2* and *p53* in caused inhibition of the rostral wave of the CNC (data not shown) by 48 hpf, which by 96 hpf resulted in malformation of jaw cartilage and muscle and loss of pharyngeal arch formation (compare Figs. 9A, 9B and 9E, 9F; see also Fig. 8C). Because of their smaller eyes, the insertions of the EOM onto the globe were more closely spaced in the *raldh2/p53* knockdown embryos (Fig. 9B), and the medial rectus had disorganized myofibers (Fig. 8F).

In contrast to MO knockdown of *raldh2*, embryos injected with MO directed against *raldh3* had no apparent jaw, pharyngeal arch, EOM, or ocular abnormalities and appeared morpho-

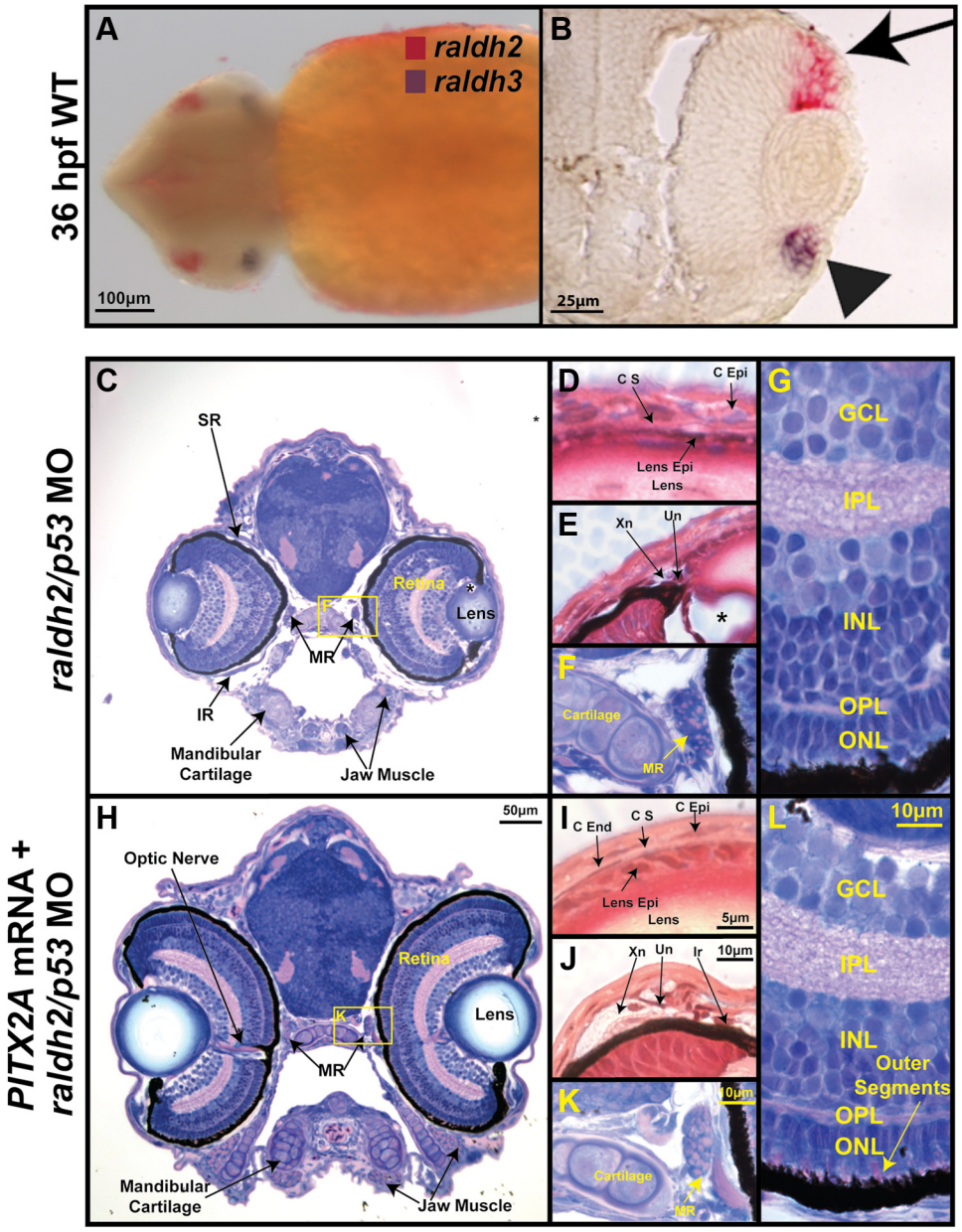

Figure 8. RA is produced by the developing eye, and human *PITX2A* mRNA rescues ocular defects caused by RA deficiency. Whole mount (**A**) and section (**B**) double in situ hybridization in 36-hpf wild-type embryos showed expression of *raldh2* (*pink*, *arrows*) predominantly in the anterodorsal retina and *raldh3* (*purple*, *arrowhead*) in the posteroventral retina in the developing eye. *Raldh2* was also expressed in the brain around the ventricles. Coronal plastic sections of 96-hpf embryos injected at the one- to two-cell stage with antisense oligonucleotide MO directed against *raldh2* and *p53* MO (**C–G**) demonstrated small and malformed eyes and deformed jaw cartilage and muscles. High magnification and trichrome-like stain of *raldh2/p53* MO knockdown embryos (**D**) revealed a thickened cornea with a scalloped epithelium (C Epi) and lack of endothelium (C End) and a dorsal iridocorneal angle (**E**) that contained fewer iris stromal cells. Cross-section of the MR in *raldh2/p53* MO (**F**) demonstrated thickening of the muscle and disorganization of the myofibers (**K**). High magnification of the developing retina in *raldh2/p53* MO knockdowns (**G**) demonstrated mild disorganization of the INL, poor demarcation of the OPL, and lack of photoreceptor outer segment formation. Coinjection with *raldh2/p53* MO and human *PITX2A* mRNA at the one-cell stage revealed restoration of ocular and jaw development (**H**). Human *PITX2A* mRNA rescued corneal architecture (**I**), dorsal iridocorneal angle structure (**J**), MR muscle, and myofiber morphology (**K**), and retinal development (**L**) in *raldh2/p53* MO knockdown embryos. SR, superior rectus; MR, medial rectus; C Epi, corneal epithelium; C S, corneal stroma; C End, corneal endothelium; Lens Epi, lens epithelium; Xn, xanthophore; Ir, iridophore; Un, undifferentiated cell; GCL, ganglion cell layer; IPL, inner plexiform layer; INL, inner nuclear layer; OPL, outer plexiform layer; ONL, outer nuclear layer.

logically similar to controls (data not shown). Coinjection of *raldh2*, *raldh3*, and *p53* MO, however, resulted in global developmental arrest, with death by 96 hpf.

Pitx2 Partially Mediates RA Regulation of Ocular and Neural Crest Development

We took advantage of our in vivo zebrafish model to assess the functional significance of the regulation of periocular *pitx2a* by RA during ocular and craniofacial development. We coinjected human *PITX2A* mRNA with *raldh2/p53* MO at the one-cell stage and found that at 96 hpf, human *PITX2A* mRNA rescued the ocular phenotype of the *raldh2/p53* MO (compare Figs. 8H and 8C), including the ocular dimensions (Table 1), corneal architecture (Fig. 8I), angle cellularity (Fig. 8J), and retinal formation (Fig. 8L). Furthermore, human *PITX2A* mRNA partially rescued the jaw and pharyngeal arch cartilage phenotypes of *raldh2*/p53 knockdown (compare Figs. 9A and 9C). Similarly, human *PITX2A* mRNA restored jaw and pharyngeal arch muscle formation in *raldh2/p53* knockdown (compare Figs. 9B and Fig. 9D).

We next sought to determine whether RA was not only necessary but sufficient for directing these events during embryogenesis. This was accomplished by replacing the developing eye with an ion-exchange bead soaked in RA. One eye was enucleated at 16 hpf; this was followed by implantation of a 40- to 60-μm ion exchange bead soaked in DMSO or 100 nM RA. Similar to previous reports,[38,44] we found that enucleation inhibited CNC and EOM development. Implantation of an RA-soaked bead into an empty orbit did not rescue either CNC development or EOM organization (data not shown).

These findings suggest that RA produced by the developing eye regulates *pitx2* expression in the periocular mesenchyme and that both RA and *pitx2* are key components in ocular and craniofacial development. RA alone, however, is not sufficient for properly organizing the orbit around the eye, demonstrating that additional signaling pathways are also required for craniofacial development.

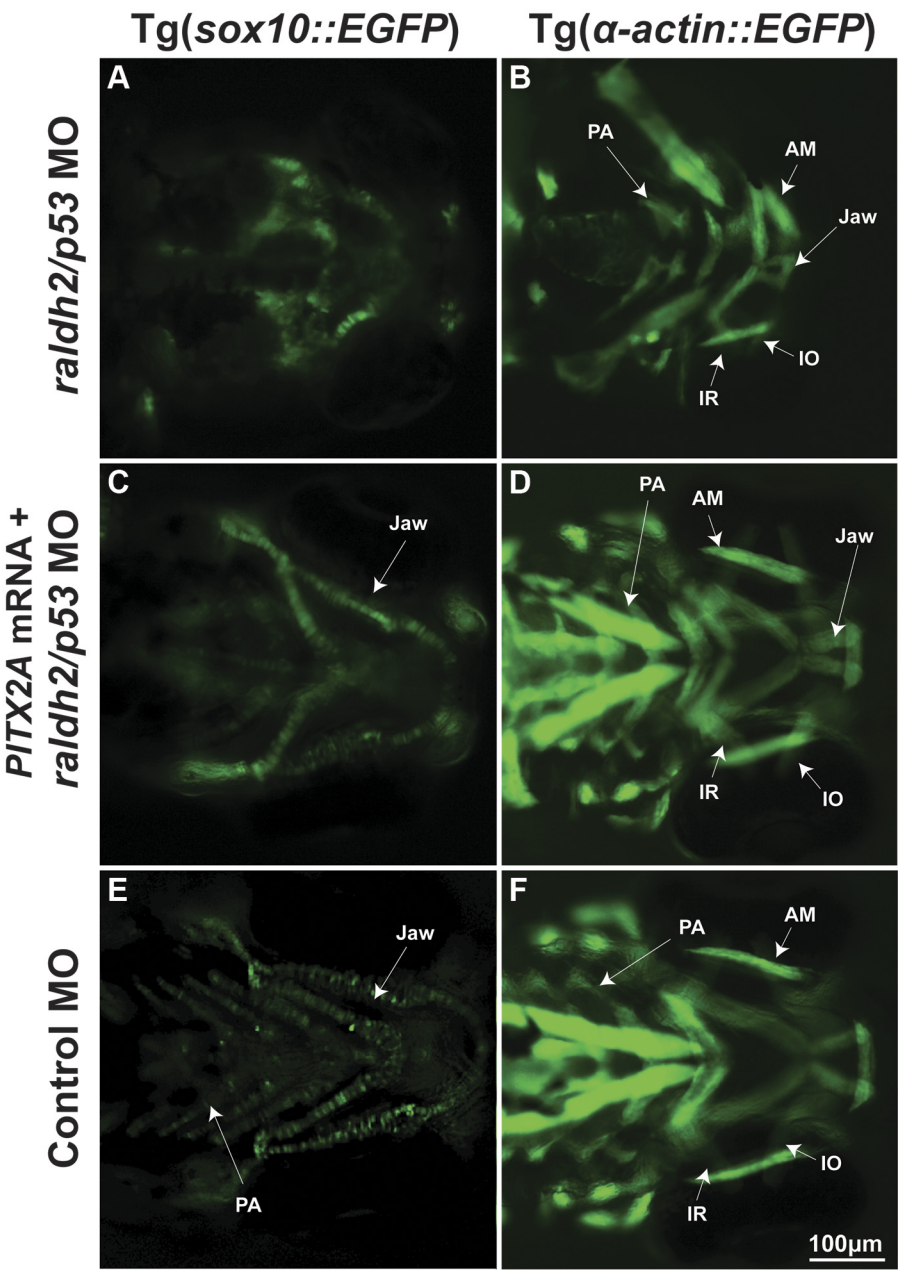

Figure 9. RA regulates zebrafish craniofacial CNC and muscle development. Microinjection of MO directed against *raldh2* and *p53* at the one- to two-cell stage into Tg(*sox10::EGFP*) embryos demonstrated inhibition of neural crest development (**A**) at 96 hpf. In the *raldh2/p53* MO knockdown, there was absence of neural crest-derived jaw and PA formation compared with embryos injected with control MO (**E**). Knockdown of *raldh2* and *p53* in Tg(*α-actin::EGFP*) embryos revealed deformed jaw and PA musculature formation (**B**) compared with control embryos (**F**). The EOMs properly differentiated, but the insertions on the globe were spaced more closely together in the *raldh2/p53* knockdown because of the smaller eye (**B**). Injection of human *pitx2a* mRNA in Tg(*sox10::EGFP*) and Tg(*α-actin::EGFP*) embryos demonstrated partial rescue of jaw and PA cartilage (**C**) and muscle (**D**) defects in *raldh2/p53* MO. PA, pharyngeal arch; IR, inferior rectus; IO, inferior oblique; AM, anterior mandibulae.

Discussion

Vertebrate craniofacial development involves complex signaling between the CNC and the surrounding tissues, and disruption of these signals during embryogenesis can result in congenital craniofacial and ocular anomalies such as those found in ARS. In the present study, we used zebrafish to investigate the function and regulation of *pitx2,* a paired-homeobox transcription factor that is commonly mutated in ARS. We first established that our zebrafish system could be used as a model for craniofacial and ocular development by recapitulating many of the characteristics of ARS by knocking down *pitx2a* expression.[3,4,49,65,66] Moreover, by rescuing phenotypes using the human form of *PITX2A* mRNA, these experiments demonstrate remarkable functional homology of *pitx2* between teleost fish and mammals and provide further evidence that similar signaling pathways are used during craniofacial and ocular development across vertebrate classes. The partial nature of the rescue may be related to the fact that injected *PITX2A* mRNA may be present in every cell in the embryo, which is, of course, abnormal in and of itself. We also expressed known disease-causing alleles of *PITX2A* and demonstrated their significance in vivo.[46–49] The K50E mutant *PITX2* gene product has an altered affinity for the DNA-binding site and can act in a dominant negative fashion by preventing wild-type *PITX2* from activating gene transcription.[72,73] Microinjection of the K50E mutant human *PITX2A* mRNA did not cause significant ocular abnormalities but did disrupt CNC development, possibly reflecting the dissimilar availability of transcriptional cofactors in the different cell populations. Furthermore, coinjection of the dominant negative mutant mRNA with *pitx2a* MO resulted in a worse ocular and neural crest phenotype than injection of either the mutant mRNA or the MO alone, uncovering in this model that graduated levels of haploinsufficiency correlate with phenotypic expressivity. These results recapitulated in zebrafish the sensitivity of the phenotypes to relative *pitx2a* expression levels in the context of this dominantly inherited

mutant allele.[46,47,49] On the other hand, the recessive T30P mutant *PITX2* gene product lacks transactivation ability but does not interfere with wild-type *PITX2* activity.[46–49,72,73] The T30P mutant human *PITX2A* mRNA did not induce significant defects when injected alone and was incapable of rescuing the *pitx2a* knockdown phenotypes, maintaining its recessive character in our zebrafish model.

Both gain-of-function and loss-of-function mutations in *PITX2* are associated with ARS,[3–8,49,65,66] and our results demonstrate the importance of tightly regulating *pitx2a* expression in both craniofacial and ocular development. In the eye, alterations in *pitx2a* expression resulted in impairment of corneal development and absence of neural crest-derived corneal endothelial and iris stromal cells. We found that in zebrafish embryos, alterations in *pitx2a* expression resulted in thicker corneas, whereas a study in humans and mice found that mutation in *PITX2* caused thinned corneas in adulthood.[64] This difference may be due to the fact that our studies examined the embryonic stage during which the corneal architecture is still being formed. The observed delay in retinal development may be secondary to a general delay in ocular development or may reveal a role for *pitx2* in retinal development. *Pitx2* has been reported to regulate optic stalk formation in a mouse model,[15] whereas a role for *pitx2* in retinal development has not previously been described. Interestingly, alterations in *pitx2a* expression were associated with arrest of retinal development at 48 hpf; *pitx2* expression around the eye peaks at 48 hpf. Further studies will be required to fully assess the role of *pitx2* in retinal development.

In our studies, alterations in *pitx2a* expression also caused abnormalities in jaw and pharyngeal arch cartilage and muscle formation. This correlates to studies in the mouse as well as the observation that patients with mutations in *PITX2* more frequently have associated craniofacial dysmorphism compared with mutations in other ARS-causing genes such as *FOXC1* and *PAX6*.[4,17–19] Thus, our data are consistent with the causative role of *pitx2* mutations in ARS and recapitulate many aspects of ARS.

In mouse models, conditional knockout of *Pitx2* disrupts development of the EOMs, and *pitx2* has been shown to activate a cascade of muscle-specific transcription factors.[14–16] In evaluating *pitx2* expression patterns, we found that *pitx2* colocalized with the muscle-specific transcript *myoD* in the periocular mesenchyme. However, despite its expression pattern and effect on jaw and pharyngeal muscles, altering *pitx2a* expression did not drastically affect development of the EOMs, although it did cause mild disorganization of the myofibers. It may be that other *pitx2* isoforms or even *pitx3* expression in EOM can compensate for the reduction in *pitx2a* expression.[76] Further studies are required to evaluate the role of *pitx2* in EOM formation and the way in which this process may differ from muscle development in other craniofacial regions in the zebrafish and myogenesis in mammalian models.

Despite its link to ARS and the essential role of *pitx2* in ocular and craniofacial development, little is known about the regulation of its expression. It has been shown that RA regulates *pitx2* expression in the periocular mesenchyme in mice, and, indeed, the *pitx2* promoter contains an RA response element.[45] However, the in vivo significance of this is difficult to assess in mammalian models. By treating embryos with exogenous RA or the inhibitor DEAB at 24 to 28 hpf, we focused the treatments to late stages of embryogenesis with the goal of avoiding broad disruptions to early embryonic patterning. We found that in zebrafish embryos, RA regulated *pitx2* expression not only in the periocular mesenchyme but also in the jaw and pharyngeal arches. Treatment of embryos with exogenous RA increased *pitx2* expression in these regions, whereas inhibition of RA synthesis by DEAB decreased *pitx2* expression. It is important to note that *pitx2* expression in the brain had the opposite response to changes in RA levels. By adding the pharmacologic agents later in embryo development, we attempted to reduce their effects on embryo patterning, which is primarily completed by 24 hpf. Using the zebrafish model, we were able to demonstrate in vivo that *pitx2* is a functional downstream target of RA in ocular and craniofacial development because injection of human *PITX2A* mRNA partially rescued the ocular and craniofacial morphogenesis defects caused by knockdown of *raldh2*. Thus, human *PITX2A* mRNA partially bypassed the RA requirement for proper development. The incomplete nature of the rescue is likely the result of additional RA-sensitive genes that are important in craniofacial morphogenesis, both known and unknown, and a reflection of the challenge of providing the precise amount of pitx2a that will lead to optimal rescue.

RA is recognized as both an essential morphogen and a teratogen that regulates craniofacial development in vertebrates. Numerous studies have demonstrated complex local regulation of RA concentration by synthesis through raldh and degradation by cyp26. Previous studies in the mouse have shown that the developing ocular tissues express *raldh2, raldh3,* and *raldh4*, as well as *cyp26*, in a precise temporal-spatial manner, which creates an RA gradient that targets periocular tissues.[27–30,77] We demonstrate that a similar process occurs in zebrafish development. Dehydrogenase enzymes expressed in the developing retina indicate the eye serves as a source of RA in the craniofacial region. Periocular, jaw, and pharyngeal arch structures displayed different sensitivities to RA that were consistent with the distance from the source of RA and the expression of degradation enzymes. The pharyngeal arches had the narrowest window of RA sensitivity, which correlates with the anatomic distance from the eye and the predominant expression of *cyp26a1* in the posterior pharyngeal arches. EOMs, on the other hand, had high tolerance to variations in RA levels, whereas the jaw had intermediate tolerance to changes in RA levels.

In addition to the sequence homology (Supplementary Fig. S5, http://www.iovs.org/lookup/suppl/doi:10.1167/iovs.11-8494/-/DCSupplemental), the functional homology of human and zebrafish *pitx2* underlies its critical role in craniofacial development and the importance of craniofacial and ocular structures in vertebrate evolution. Indeed, even blind and grossly eyeless fish have maintained primordial eye structures buried within the facial skeleton that may interact with signaling centers in generating proper craniofacial structures.[39] The evolutionary conservation of RA and *pitx2* function in the context of significant differences in craniofacial structures represents remarkable modularity of the gene networks that are responsible for vertebrate morphogenesis. Similarly, despite the significant differences between human and zebrafish anterior segments, the same genes and signals appear to play key roles in ocular development. This suggests that the zebrafish model of ARS may be useful for not only studying this genetic disorder but for using certain strengths of the zebrafish model, such as high throughput screening, to develop novel therapies.

In summary, we report that, in zebrafish, *pitx2* is a downstream target of RA and that together *pitx2* and RA mediate signals among the developing eye, CNC, and surrounding tissues to regulate ocular and craniofacial development. Furthermore, zebrafish *pitx2* and human *PITX2* share significant functional homology, revealing a remarkable conservation of function between teleost fish and humans that may prove to be useful in generating novel therapies for human RA- and *PITX2*-related disorders.

Acknowledgments

The authors thank Rose Elsaeidi, Donika Gallina, and Steven Grzegorski for technical assistance; Mitchell Gillett for tissue processing, sectioning, and staining of the methyl acrylate ocular sections; Phillip Gage and Peter Hitchcock for critical reading of the manuscript; and Michael Walter, Rachel Wong, and Phillip Gage for sharing reagents.

References

1. Idrees F, Bloch-Zupan A, Free SL, et al. A novel homeobox mutation in the *PITX2* gene in a family of Axenfeld-Rieger syndrome associated with brain, ocular, and dental phenotypes. *Am J Med Genet B Neuropsychiatr Genet.* 2006;141B:184–191.
2. Dressler S, Meyer-Marcotty P, Weisschuh N, et al. Dental and craniofacial anomalies associated with Axenfeld-Rieger syndrome with PITX2 mutation. *Case Report Med.* 2010;2010:621984.
3. Tumer Z, Bach-Holm D. Axenfeld-Rieger syndrome and spectrum of Pitx2 and Foxc1 mutations. *Eur J Hum Genet.* 2009;17:1527–1539.
4. Hjalt TA, Semina EV. Current molecular understanding of Axenfeld-Rieger. *Expert Rev Mol Med.* 2005;7:1–17.
5. Priston M, Kozlowski K, Gill D, et al. Functional analyses of two newly identified PITX2 mutants reveal a novel molecular mechanism for Axenfeld Rieger syndrome. *Hum Mol Genet.* 2001;10:1631–1638.
6. Phillips JC. Four novel mutations in the *PITX2* gene in patients with Axenfeld-Rieger syndrome. *Ophthalmic Res.* 2002;34:324–326.
7. Lines MA, Kozlowski K, Kulak SC, et al. Characterization and prevalence of PITX2 microdeletions and mutations in Axenfeld-Rieger malformations. *Invest Ophthalmol Vis Sci.* 2004;45:828–833.
8. Saadi I, Toro R, Kuburas A, Semina EV, Murray JC, Russo AF. An unusual class of PITX2 mutations in Axenfeld-Rieger syndrome. *Birth Defects Res A Clin Mol Teratol.* 2006;76:175–181.
9. Semina EV, Reiter R, Leysens NJ, et al. Cloning and characterization of a novel bicoid-related homeobox transcription factor gene, RIEG, involved in Rieger syndrome. *Nat Genet.* 1996;14:392–399.
10. Cox CJ, Espinoza HM, McWilliams B, et al. Differential regulation of gene expression by PITX2 isoforms. *J Biol Chem.* 2002;277:25001–25010.
11. Essner JJ, Branford WW, Zhang J, Yost HJ. Mesendoderm and left-right brain, heart and gut development are differentially regulated by pitx2 isoforms. *Development.* 2000;127:1081–1093.
12. Evans AL, Gage PJ. Expression of the homeobox gene Pitx2 in neural crest is required for optic stalk and ocular anterior segment development. *Hum Mol Genet.* 2005;14:3347–3359.
13. Kitamura K, Miura H, Miyagawa-Tomita S, et al. Mouse Pitx2 deficiency leads to anomalies of the ventral body wall, heart, extra- and periocular mesoderm and right pulmonary isomerism. *Development.* 1999;126:5749–5758.
14. Diehl AG, Zareparst S, Qian M, Khanna R, Angeles R, Gage PJ. Extraocular muscle morphogenesis and gene expression are regulated by Pitx 2 gene dose. *Invest Ophthalmol Vis Sci.* 2006;47:1785–1793.
15. Zacharias AL, Lewandoski M, Rudnicki MA, Gage PJ. Pitx2 is an upstream activator of extraocular myogenesis and survival. *Dev Biol.* 2011;349:395–405.
16. Zhou Y, Cheng G, Dieter L, et al. An altered phenotype in a conditional knockout of pitx2 in extraocular muscle. *Invest Ophthalmol Vis Sci.* 2009;50:4531–4541.
17. Dong F, Sun X, Liu W, et al. Pitx2 promotes development of splanchnic mesoderm-derived branchiomeric muscle. *Development.* 2006;133:4891–4899.
18. Liu W, Selever J, Lu MF, Martin JF. Genetic dissection of Pitx2 in craniofacial development uncovers new functions in branchial arch morphogenesis, late aspects of tooth morphogenesis and cell migration. *Development.* 2003;130:6375–6385.
19. Shih HP, Gross MK, Kloussi C. Cranial muscle defects of Pitx2 mutants result from specification defects in the first branchial arch. *Proc Nat Acad Sci U S A.* 2007;104:5907–5912.
20. Sandell LL, Sanderson BW, Moiseyev G, et al. RDH10 is essential for synthesis of embryonic retinoic acid and is required for limb, craniofacial, and organ development. *Genes Dev.* 2007;21:1113–1124.
21. Lampert JM, Holzschuh J, Hessel S, Driever W, Vogt K, von Lintig J. Provitain A conversion to retinal via the beta,beta-carotene-15,15′-oxygenase (bcox) is essential for pattern formation and differentiation during zebrafish embryogenesis. *Development.* 2003;130:2173–2186.
22. Gitton Y, Heude E, Vieux-Rochas M, et al. Evolving maps in craniofacial development. *Semin Cell Dev Biol.* 2010;21:301–308.
23. Deltour L, Ang HL, Duester G. Ethanol inhibition of retinoic acid synthesis as a potential mechanism for fetal alcohol syndrome. *FASEB J.* 1996;10:1050–1057.
24. Shean ML, Duester G. The role of alcohol dehydrogenase in retinoic acid homeostasis and fetal alcohol syndrome. *Alcohol Alcohol Suppl.* 1993;2:51–56.
25. de la Cruz E, Sun S, Vangvanichyakorn K, Desposito F. Multiple congenital malformations associated with maternal isotretinoin therapy. *Pediatrics.* 1984;74:428–430.
26. Rosa FW, Wilk AL, Felsey FO. Teratogen update: vitamin A congeners. *Teratology.* 1986;33:355–364.
27. Suzuki R, Shintani T, Sakuta H, et al. Identification of RALDH-3 a novel retinaldehyde dehydrogenase, expressed in the ventral region of the retina. *Mech Dev.* 2000;98:37–50.
28. Molotkov A, Molotkova N, Duester G. Retinoic acid guides eye morphogenetic movements via paracrine signaling but is unnecessary for retinal dorsoventral patterning. *Development.* 2006;133:1901–1910.
29. McCaffery P, Wagner E, O'Neil J, Petkovich M, Drager UC. Dorsal and ventral retinal territories defined by retinoic acid synthesis, break-down and nuclear receptor expression. *Mech Dev.* 1999;82:119–130.
30. Hernandez RE, Putzke AP, Myers JP, Margaretha L, Moens CB. Cyp26 enzymes generate the retinoic acid response pattern necessary for hindbrain development. *Development.* 2007;134:177–187.
31. Matt N, Dupe V, Garnier J-M, et al. Retinoic acid-dependent eye morphogenesis is orchestrated by neural crest cells. *Development.* 2005;132:4789–4800.
32. Matt N, Ghyselinck NB, Pellerin I, Dupe V. Impairing retinoic acid signalling in the neural crest cells is sufficient to alter entire eye morphogenesis. *Dev Biol.* 2008;320:140–148.
33. Matt N, Ghyselinck NB, Wendling O, Chambon P, Mark M. Retinoic acid-induced developmental defects are mediated by RAR-beta/RXR heterodimers in the pharyngeal endoderm. *Development.* 2003;130:2083–2093.
34. Hale LA, Tallafuss A, Yan YL, Dudley L, Elsen JS, Postlethwait JH. Characterization of the retinoic acid receptor genes raraa, rarab and rarg during zebrafish development. *Gene Expr Patterns.* 2006;6:546–555.
35. Bertrand S, Thisse B, Tavares R, et al. Unexpected novel relational links uncovered by extensive developmental profiling of nuclear receptor expression. *PLoS Genet.* 2007;3(11):e188.
36. Rauch GJ, Lyons DA, Middendorf I, et al. Submission and curation of gene expression data. ZFIN Direct Data Submission. ZFIN ID: ZDB-PUB-031103–24, 2003. Available at http://zfin.org. Accessed December 19, 2011 (using 'rar' as the keyword).
37. Bolande RP. The neurocristopathies: a unifying concept of disease arising in neural crest maldevelopment. *Hum Path.* 1974;5:409–429.
38. Bohnsack BL, Gallina D, Thompson H, et al. Development of extraocular muscles requires early signals from periocular neural crest and the developing eye. *Arch Ophthalmol.* 2011;129(8):1030–1041.
39. Kish PE, Bohnsack BL, Gallina D, Kasprick DS, Kahana A. The eye as an organizer of craniofacial development. *Genesis.* 2011;49:222–230.
40. Trainor PA, Tam PPL. Cranial paraxial mesoderm and neural crest of the mouse embryo-codistribution in the craniofacial mesenchyme but distinct segregation in the branchial arches. *Development.* 1995;121.

41. Trainor PA, Krumlauf R. Patterning the cranial neural crest: hindbrain segmentation and Hox gene plasticity. *Nat Rev Neurosci.* 2000;1:116–124.
42. Noden DM. The role of the neural crest in patterning of avian cranial skeletal, connective, and muscle tissues. *Dev Biol.* 1983; 96:144–165.
43. Noden DM. Cell movements and control of patterned tissue assembly during craniofacial development. *Am J Anat.* 1991;168: 257–276.
44. Langenberg T, Kahana A, Wszalek JA, Halloran MC. The eye organizes neural crest cell migration. *Dev Dyn.* 2008;237:1645–16521.
45. Kumar S, Duester G. Retinoic acid signaling in perioptic mesenchyme represses Wnt signaling via induction of Pitx2 and Dkk2. *Dev Biol.* 2010;340:67–74.
46. Chaney BA, Clark-Baldwin K, Dave V, Ma J, Rance M. Solution structure of the K50 class homeodomain PITX2 bound to DNA and implications for mutations that cause Rieger syndrome. *Biochemistry.* 2005;44:7497–7511.
47. Saadi I, Kuburas A, Engle JJ, Russo AF. Dominant negative dimerization of a mutant homeodomain protein in Axenfeld-Rieger syndrome. *Mol Cell Biol.* 2003;23:1968–1982.
48. Amendt BA, Sutherland LB, Semina EV, Russo AF. The molecular basis of Rieger syndrome: Analysis of Pitx2 homeodomain protein activities. *J Biol Chem.* 1998;273:20066–20072.
49. Kozlowski K, Walter MA. Variation in residual PITX2 activity underlies the phenotypic spectrum of anterior segment developmental disorders. *Hum Mol Genet.* 2000;9:2131–2139.
50. Kimmel CB, Ballard WW, Kimmel SR, Ullmann BB, Schilling TF. Stages of embryonic development of the zebrafish. *Dev Dyn* 1995; 203:253–310.
51. Dutton K, Dutton JR, Pauliny A, Kelsh RN. A morpholino phenocopy of the colourless mutant. *Genesis.* 2001;30:188–189.
52. Wada N, Javidan Y, Nelson S, Carney TJ, Kelsh RN, Schilling TF. Hedgehog signaling is required for cranial neural crest morphogenesis and chondrogenesis at the midline in the zebrafish skull. *Development.* 2005;132:3977–3988.
53. Higashijima S, Okamoto H, Ueno N, Hotta Y, Eguchi G. High-frequency generation of transgenic zebrafish which reliably express GFP in whole muscles or the whole body by using promoters of zebrafish origin. *Dev Biol.* 1997;192:289–299.
54. White RM, Sessa A, Burke C, et al. Transparent adult zebrafish as a tool for in vivo transplantation analysis. *Cell Stem Cell.* 2008;2: 183–189.
55. Karlsson J, von Hofsten J, Olsson P-E. Generating transparent zebrafish: a refined method to improve detection of gene expression during embryonic development. *Mar Biotechnol.* 2001;3: 522–527.
56. Barthel LK, Raymond PA. In situ hybridization studies of retinal neurons. *Methods Enzymol.* 2000;316:579–590.
57. Prophet EB, Mills B, Arrington JB, Sobin LH, eds. *Laboratory Methods in Histotechnology*. Washington, DC: American Registry of Pathology; 1992.
58. Gruber HE. Adaptations of Goldner's Masson trichrome stain for the study of undecalcified plastic embedded bone. *Biotechnic Histochem.* 1992;67:30–34.
59. Begemann G, Schilling TF, Rauch G-J, Geisler R, Ingham PW. The zebrafish neckless mutation reveals a requirement for raldh2 in mesodermal signals that pattern the hindbrain. *Development.* 2001;128:3081–3094.
60. Langheinrich U, Hennen E, Stott G, Vacun G. Zebrafish as a model organism for identification and characterization of drugs and genes affecting p53 signaling. *Curr Biol.* 2002;12:2023–2028.
61. Ma AC, Chung MI, Liang R, Leung AY. A DEAB-sensitive aldehyde dehydrogenase regulates hematopoietic stem and progenitor cells development during primitive hematopoiesis in zebrafish embryos. *Leukemia.* 2010;24:2090–2099.
62. Berry FB, Lines MA, Ooas JM, et al. Functional interactions between FOXC1 and PITX2 underlie the sensitifvity to FOXC! gene dose in Axenfeld-Rieger syndrome and anterior segment dysgenesis. *Hum Mol Genet.* 2006;15:905–919.
63. White RJ, Nie Q, Lander AD, Schilling TF. Complex regulation of cyp26a1 creates a robust retinoic acid gradient in the zebrafish embryo. *PLoS Biol.* 2007;5:e304.
64. Asai-Coakwell M, Backhouse C, Casey RJ, Gage PJ, Lehmann OJ. Reduced human and murine corneal thickness in an Axenfeld-Rieger Syndrome subtype. *Invest Ophthalmol Vis Sci.* 2006;47: 4905–4909.
65. Kulak SC, Kozlowski K, Semina EV, Pearce WG, Walter MA. Mutation in the *RIEG1* gene in patients with iridogoniodysgenesis syndrome. *Hum Mol Genet.* 1998;7:1113–1117.
66. Pearce WG, Mielke BC, Kulak SC, Walter MA. Histopathology and molecular basis of iridogoniodysgenesis syndrome. *Ophthalmic Genet.* 1999;20:83–88.
67. Soules KA, Link BA. Morphogenesis of the anterior segment in the zebrafish eye. *BMC Dev Biol.* 2005;5:12.
68. Dutton KA, Pauliny A, Lopes SS, et al. Zebrafish colourless encodes sox10 and specifies non-ectomesenchymal neural crest fates. *Development.* 2001;128:4113–4125.
69. Curran K, Raible DW, Lister JA. Foxd3 controls melanophore specification in the zebrafish neural crest by regulation of Mitf. *Dev Biol.* 2009;332:408–417.
70. Simard A, Di Giorgio L, Amen M, Westwood A, Amendt BA, Ryan AK. The Pitx2c N-terminal domain is a critical interaction domain required for asymmetric morphogenesis. *Dev Dyn.* 2009;238: 2459–2470.
71. Yu X, St Amand TR, Wang S, et al. Differential expression and functional analysis of Pitx2 isoforms in regulation of heart looping in the chick. *Development.* 2001;128:1005–1013.
72. Banerjee-Basu S, Baxevanis AD. Threading analysis of the Pitx2 homeodomain: predicted structural effects of mutations ausing Rieger syndrome and iridogoniodysgenesis. *Hum Mutation.* 1999; 14:312–319.
73. Saadi I, Semina EV, Amendt BA, et al. Identification of a dominant negative homeodomain mutation in Rieger syndrome. *J Biol Chem.* 2001;276:23034–23041.
74. Barembaum M, Bronner-Fraser M. Early steps in neural crest specification. *Sem Cell Dev Biol.* 2005;16:642–646.
75. Steventon B, Carona-Fontaine C, Mayor R. Genetic network during neural crest induction: from cell specification to cell survival. *Sem Cell Dev Biol.* 2005;16:647–654.
76. L'Honore A, Coulon V, Marcil A, et al. Sequential expression and redundancy of Pitx2 and Pitx3 genes during muscle development. *Dev Biol.* 2007;307:432–433.
77. Wagner E, McCaffery P, Drager UC. Retinoic acid in the formation of the dorsoventral retina and its central projections. *Dev Biol.* 2000;222:460–470.